

B O U N D A R Y L A Y E R O B S E R V A T I O N S
O V E R T H E O C E A N S

B Y

E R N S T A U G S T E I N
M A X - P L A N C K I N S T I T U T F Ü R M E T E O R O L O G I E , H A M B U R G
F E D E R A L R E P U B L I C O F G E R M A N Y

1. Introduction

Observational studies basically serve three purposes. Firstly, they are important to explore and quantitatively document natural facts in order to stimulate satisfactory theoretical description of the findings. Secondly, experiments are necessary in order to determine constants or coefficients which are universal for certain materials and/or geometrical conditions. Finally, measurements are required for verification of simplified model hypotheses which are unavoidable in a practical treatment of the complex atmosphere-hydrosphere-solid earth system. Fulfilling this task is most complicated in regions where the different media interact with each other, namely the so-called boundary layers. Allowing for a certain vagueness we may use the term atmospheric boundary layer (ABL) for the lower part of the atmosphere where the frictional and the thermal effects of the underlying surface directly modify the mean air flow. Thus, the structure of the ABL will mainly depend upon the hydrodynamical roughness of and the energy transfer across the lower boundary. Sometimes the exchange of chemical substances such as aerosols and gases may also influence the physical properties of the boundary layer air flow.

From these statements which are based on observations and theoretical considerations one may suspect that variations of the terrain and particularly the differences between land and the sea surfaces will be reflected in the behaviour of the atmospheric boundary layer. In this respect it is of great importance that the atmospheric motion generates surface waves and drift currents in the ocean both of which contribute to a turbulent vertical mixing in the upper part of the water body. As a consequence, a boundary layer, the so called "mixed layer" also develops in the ocean. The drift currents, in addition to promoting vertical mixing also produce considerable horizontal transports of energy and momentum. Further differences between the maritime and the continental ABL also result from the differences between water and land with respect to heat capacity and propagation depths of solar radiation. And finally, the oceans can be regarded as infinite water vapour reservoirs while the water content of soil can considerably vary in time and space.

Thus, a separate treatment of the ABL over water, land and - in order to be complete - ice surfaces seems to be reasonable. As the development of the boundary layers in ocean and atmosphere are closely coupled, a fully sufficient investigation of the air-sea interaction processes stipulates a simultaneous study of both media. This restraint can only be dropped if due to the different time scales of the atmospheric and oceanic processes back-coupling effects are negligibly small. Therefore, observations of the marine ABL should in any case include oceanic parameters such as sea-surface temperature and surface current as well as some gross information about surface waves in order to examine the limitations of the particular study.

2. Current experimental techniques for maritime ABL studies

Physical properties of the lower atmosphere can basically be measured through direct or indirect probing. The first method provides data of "in situ" sensors while the second technique processes signals which are either actively emitted by the medium or result from well understood modifications of artificially induced signals by the atmosphere and the ocean.

It would be beyond the frame of this lecture to discuss observational techniques in detail but it might be useful to briefly indicate some of the frequently applied procedures.

2.1. Direct measurements

For direct sensing of atmospheric properties over the ocean the following platforms are used for carrying instruments: ships, buoys, rafts, aircraft, tethered and free rising balloons, kites and in shallow waters towers and poles. Sometimes, even small islands serve as launching bases for balloon-borne equipment. The data transfer from the sensor packages exposed on buoys, rafts, balloons or drop sondes to the recording land, ship, or aircraft stations is achieved through cable links or by radio transmission. Quantities to be measured by direct methods include air and water temperature, air pressure, humidity, wind vector, ocean currents, surface waves, solar and long wave radiation and precipitation. In addition to simple apparatus with slowly responding sensors for measuring mean values, rather sophisticated techniques have been developed in order to detect high frequency fluctuations up to 10 or even 100 Hz. Such so called flux probes - which enable the computation of the turbulent transports of heat, water vapour, and momentum as well as the relevant spectra - have been successfully applied to fixed (towers and anchored poles) as well as to moving platforms (buoys, aircraft, tethered balloons). In the latter case considerable precautions are necessary in order to eliminate the effects introduced by the platform motions.

Vertical profiles of temperature, water vapour and the wind vector throughout the entire ABL are mainly obtained from radiosondes on tethered and free-rising balloons. In the latter case tracking of the balloon by radar or theodolites or, recently, by radio navigational systems like OMEGA and LORAN-C provides the vertical wind distribution. Profiles of the relevant quantities for determination of surface fluxes are measured in the lowest meters above the sea surface from fixed towers and masts as well as from ship booms and meteorological buoys. And since satellites are available for data transmission, first attempts have been made to use constant level balloons in order to determine the horizontal trajectories of the boundary layer air flow over the open ocean.

2.2. Indirect techniques

2.2.1 Remote sensing

Remote sensing is a new means of investigating the ABL which is very promising for several reasons. Firstly, the atmospheric field will not be disturbed by any "in situ" sensor. Secondly,

the method is not restricted to point measurements but produces vertical or horizontal profiles or averages of certain parameters. Thirdly, remote sensing equipment which can be used from aircraft and satellites is able to probe large oceanic areas within a short span of time. And finally, recording of high resolution long time series is made possible and economical. Clearly, not all direct measurements will be replaceable by indirect observations and serious problems arise when high absolute accuracy is required. The most successful remote sensing technique at the present time is echo-sounding of an air volume with optical(lidar), acoustic(sodar) and high frequency radio(radar) signals. The intensity and pattern of the echo display gives qualitative insight into the turbulent structure of the ABL and provides quantitative values of cell sizes and height variations of scattering volumes. And from the Doppler frequency shift between the emitted and return signal the air motion parallel to the beam can be derived. A satisfactory application of these systems over the ocean is limited to ships which have a sufficiently vertically stabilized platform and to fixed tower stations. Among several other remote sensing methods - most of which have not yet passed the laboratory phase - the sea surface temperature and cloud top measurement through infrared radiation have been rather successful already.

2.2.2 Budget method

Under certain conditions, the small scale(sub-grid) transports of energy, water, mass, and momentum can also be derived indirectly through integration of the respective conservation laws over a given large scale (grid) volume. This budget method yields useful results if the large scale properties are linearly between the grid points and the flow is rather stationary as e.g. in undisturbed trades. A simplified form of the budget concept is the so called "ageostrophic method" for determining the vertical stress profile within the ABL from the mean wind profile and the mean horizontal pressure and temperature gradient.

3. Schematic structure of the maritime ABL

Based on experimental and model studies one may schematically describe the ABL over the ocean as sketched in Figure 1. Although considerable deviations from this idealized structure can occur it may serve quite well as a guidance for modellers and for experimental planning purposes. The most variable part within this scheme is the cloud layer. Under certain large scale flow conditions no clouds are able to form in which case the ABL terminates at the transition layer. Sometimes very deep clouds develop and extend up to the level of the tropopause; in this case the top of the ABL remains ill-defined. A one-dimensional representation of the boundary layer structure may become principally invalid in conditions with strong changes of baroclinity, due to horizontal advection and particularly in the vicinity of air mass fronts. Nevertheless, the diagram of Figure 1 is thought to be a useful starting point for the subsequent discussion.

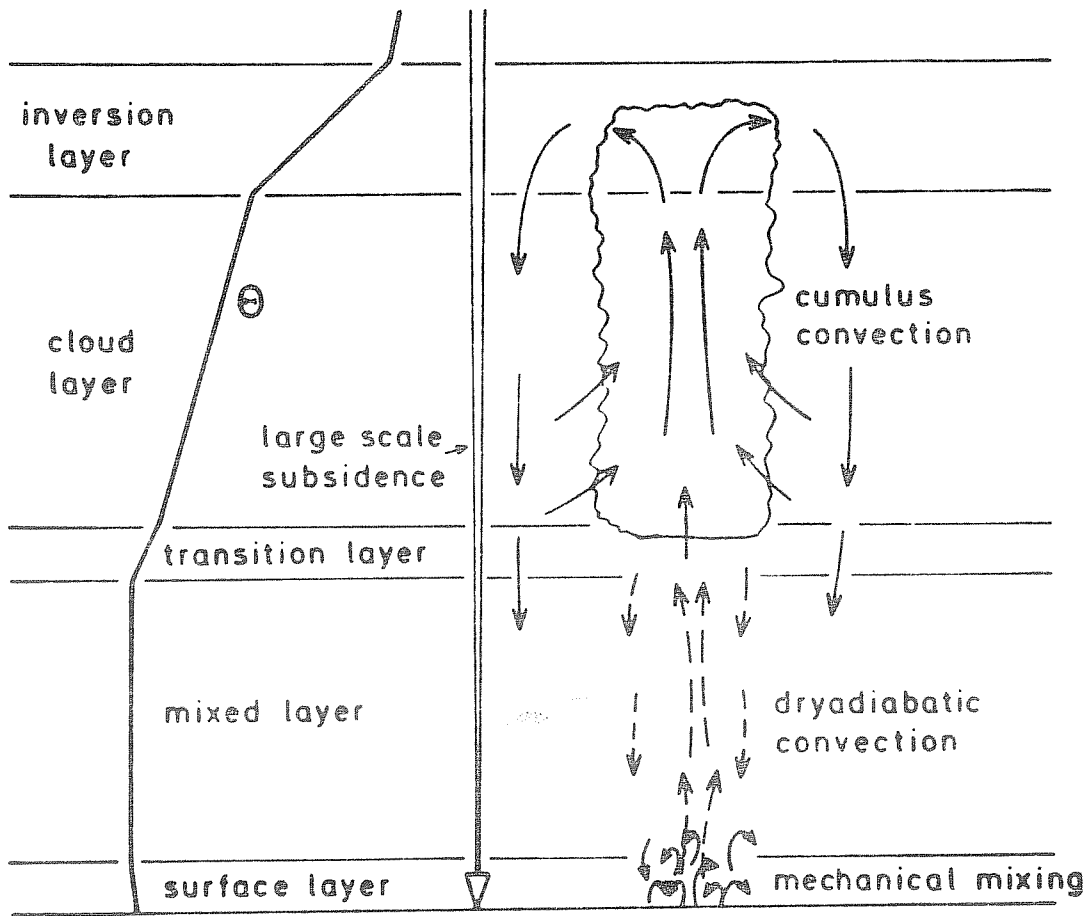


Figure 1. Scheme of dominant processes in a multilayered atmospheric boundary layer. Θ = potential temperature.

Principally, short and long wave radiation, which as a net effect cause cooling in the entire atmospheric boundary layer, should be included in this scheme. Direct interaction between the relatively short-lived turbulent and convective elements and radiation can be neglected (Sasamori, 1972), but indirect influences by radiatively caused slow changes of the mean static stability can of course modify the statistical characteristics of the small-scale motions.

In the non-precipitating trade wind belts - where our scheme fits best - radiative cooling is mainly compensated by adiabatic warming of the large-scale subsiding air and to a smaller extent by sensible heat input from the ocean. The distribution of the various processes is primarily based on observational findings. Co-spectra of momentum, heat and moisture fluxes measured by Pond et al. (1971) - shown in Figure 2 - as well as data of Wucknitz (1976) indicate that microscale turbulence is dominant in the surface layer transports. Air craft measurements of Bean et al. (1972) in Figure 3 suggest that with increasing height buoyancy-driven dry convection gains more and more importance. The buoyancy-driven mixing produces a well-mixed region above the shallow surface layer. The development of such a layer in a subsiding initially stably stratified airflow with unstable conditions only at the lower boundary has been described successfully with the aid of rather similar model assumptions by Ball (1960), Lilly (1968), Carson (1973), Tennekes (1973), and Deardorff (1972). All of these authors coincidentally imply that the buoyancy generated kinetic energy by concurrently heating and moistening of the air from below is totally (Ball, 1960) or partly (all the others) converted into potential energy through entrainment of potentially warmer air from above through the top of the mixed layer. In order to achieve this effect buoyant parcels are assumed to overshoot their level of equilibrium thereby forcing mass with smaller density downwards. Thus, the top of the mixed layer is determined by a balance of the small-scale mass entrainment from below and the large-scale downward mass flow.

As soon as the most powerful convective plumes or bubbles penetrate to their condensation level clouds start to develop. This process has been simulated in a numerical grid point model recently by Sommeria (1976). The physical processes connected with single non-precipitating clouds has been described in detail by Betts (1973). Nevertheless presently no sufficient concept exists for a satisfactory prognostic formulation of the cloud transports of heat, water vapour and momentum. Although considerable progress in this field has been achieved by Arakawa and Schubert (1974) on the one hand and Krishnamurti (1975) on the other hand several questions, especially with respect to the momentum transports and to cloud interaction, are still open.

4. The exchange processes at and near the sea surface

Most of the past experimental boundary layer work has been devoted to the lowest 20 m above the sea surface. This fact is on the one hand scientifically motivated since the exchange of energy, momentum and matter has a strong influence on the flow

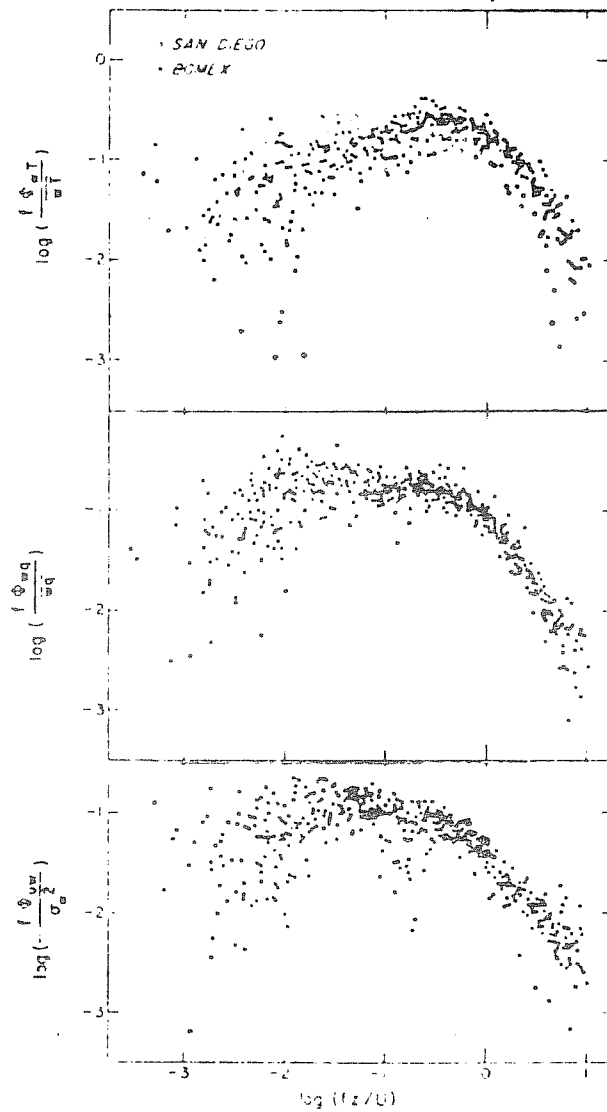


Figure 2. Normalized co-spectra of heat (above), moisture (middle), and momentum (below) observed by Pond et al. (1971).

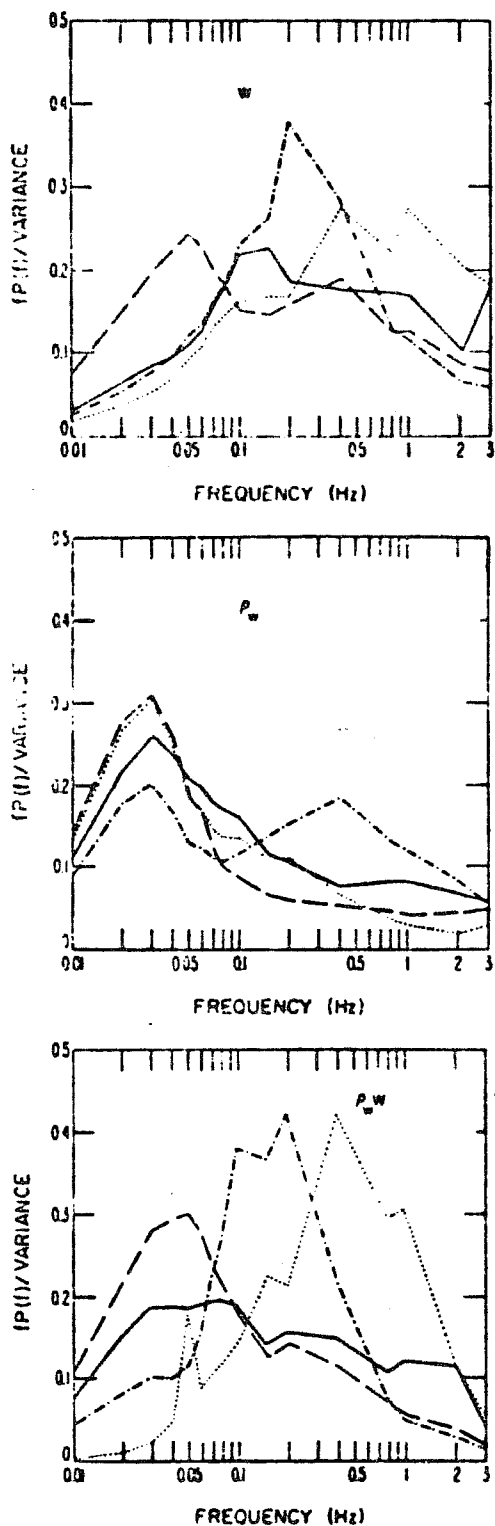


Figure 3. Spectra of vertical motion (W), water vapour density (ρ_w) and moisture flux ($\rho_w w$) during BOMEX after Bean et al. (1972). Alongwind: at 152 m long dashes, at 33 m solid line. Crosswind: at 152 m dash-dotted curve, at 33m dotted line.

field and on the thermodynamic state of the media on both sides of their interface. But on the other hand there is also a practical reason, namely that floating and fixed platforms enable instrument exposure in the easiest way in the surface layer. For determination of the energy and momentum exchange through the sea surface mainly three principles have been applied: the eddy correlation technique, the profile hypothesis and the so-called aerodynamic formulae. The aerodynamic formulae form a parameterization scheme which is also frequently used in ABL and general circulation models. In addition to the above-mentioned methods some attempts have been made to calculate the sensible heat flux from temperature gradients within the molecular layers on both sides of the sea surface.

The turbulent vertical fluxes of momentum (F_D), heat (F_θ), and water vapour (F_q) near an aerodynamical rough surface may be expressed as follows:

$$(1) \quad \tilde{F}_D = -\rho \overline{v'w'} \approx \rho K_D \frac{\partial \bar{v}}{\partial z} \approx \rho c_D \bar{v}_a \cdot \bar{v}_a$$

$$(2) \quad \tilde{F}_\theta = c_p \rho \overline{\theta'w'} \approx -c_p \rho K_\theta \frac{\partial \bar{\theta}}{\partial z} \approx c_p \rho c_\theta \Delta \bar{\theta} \cdot \bar{v}_a$$

$$(3) \quad \tilde{F}_q = \rho \overline{q'w'} \approx -\rho K_q \frac{\partial \bar{q}}{\partial z} \approx \rho c_q \Delta \bar{q} \cdot \bar{v}_a$$

In this familiar notation \bar{v} is the horizontal wind velocity, v is the wind speed, $\Delta \theta = \theta_0 - \theta_a$ and $\Delta q = q_0 - q_a$ are the differences of potential temperature and specific humidity between a reference height a and the sea surface, marked by the subscript zero.

Starting from the left side the second expressions in equations (1) to (3) represent the Reynolds notation of the fluxes, the third alternative expressions indicate the mean profile relation and the last terms are the bulk aerodynamic formulae. The non-dimensional transfer coefficients c_D, c_θ, c_q are functions of the height z , the so-called "roughness length" z_0 and the static stability of the surface layer z/L .

Thus we have

$$(4) \quad c_D, c_\theta, c_q = c_D, c_\theta, c_q \left(\frac{z}{z_0}, \frac{z}{L} \right)$$

where L is the Monin-Obukhov scaling length.

Although the physical meaning of z_0 over ocean surfaces is not yet clear, it is suggestive to imply that this parameter may be somehow related to the surface wave spectrum. Within the light

of such uncertainties it is not surprising that Charnock's (1955) relation

$$(5) \quad z_0 = m_0 \frac{u^{*2}}{g}$$

- with $u^{*2} = -\overline{v'w'}$ and $m_0 =$ proportionality coefficient - can be in remarkable disagreement with observations (Brocks and Krügermeyer, 1972). In equation (5) all undetermined problems are hidden in m_0 , which is therefore again dependent on some other dimensionless variables including wave parameters. Further effects which complicate the parameterization of the surface fluxes are wave breaking, sea spray, precipitation and oceanic variations such as cold upwelling, internal wave mixing, formation of surface films (slicks), etc. Therefore, the subsequent observations should be judged in the light of the quoted limitations. As all other methods for flux determination are based on some hypotheses we will restrict ourselves to eddy correlation measurements, despite the fact that few such measurements are available, and for comparison we will consider the relations

$$(6) \quad \begin{aligned} c_D &= \frac{\overline{v'w'}}{\overline{v \cdot v}} && \text{(momentum)} \\ c_\theta &= \frac{\overline{\theta'w'}}{\Delta\overline{\theta \cdot v}} && \text{(heat)} \\ c_q &= \frac{\overline{q'w'}}{\Delta\overline{q \cdot v}} && \text{(water vapour)} \end{aligned}$$

4.1. Momentum flux

Measurements of $\overline{v'w'}$ over the open ocean have been reported by Volkov and Kitaigorodsky (1967), Pond et al (1971) and Wucknitz (1976). Observations from platforms near the coast have been published by Weiler and Burling (1967), Smith (1967), Hasse (1968), De Leonibus (1971), Miyake et al (1970), and Garratt and Hyson (1975). The results of all of these measurements are combined in Figure 4 without regard to static stability. We follow the common procedure of relating c_D to wind speed. Kitaigorodskii's (1970) suggestion to choose the non-dimensional coordinate c_0/u^* ($c_0 =$ phase speed of dominant waves, $u^* = \sqrt{\overline{v'v'}}$) seems to be more appealing but it has two disadvantages. Firstly, c_D and u^* are not independent and secondly, it is doubtful if c_0 alone is sufficient to describe the wave spectrum for this purpose. Including the results of Smith and Banke (1975), which have been derived from measurements at a sand spit of a small island, two important conclusions can be drawn from Figure 4. At wind speeds below 10 m/sec the drag coefficient scatters around $1.3 \cdot 10^{-3}$. This value agrees roughly with derivations from profile measurements of Badgley (1972), Brocks and Krügermeyer (1972),

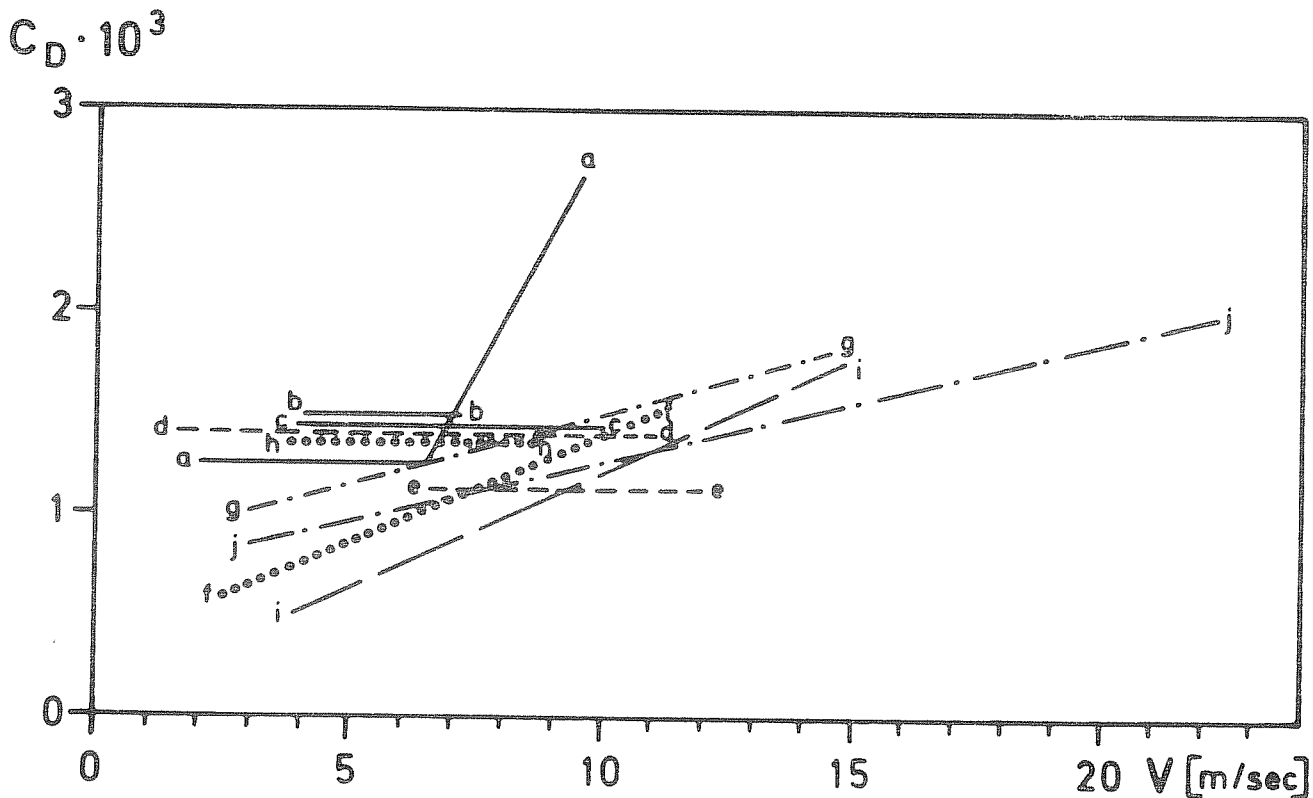


Figure 4. Drag coefficients determined for the free ocean by a) Volkov and Kitaigorodsky (1967), b) Pond et al (1971), c) Wucknitz (1976) and near the coast by d) Weiler and Burling (1967), e) Smith (1967), f) Hasse (1968), g) De Leonibus (1971), h) Miyake et al (1970), i) Garatt and Hyson (1975) and j) Smith and Banke (1975).

and Paulson (1972) for neutral static stability. And for higher wind speeds c_D seems to increase, being about $2.5 \cdot 10^{-3}$ at 25-30 m/sec wind speed. Although this tendency is confirmed by profile data of Sheppard et al (1972) and ageostrophic computations of Miller (1964), there is a great need for reliable eddy correlation measurements at wind speeds higher than 20 m/sec. We believe that a considerable reduction of the data scatter in general can only come from combined studies of surface waves and the turbulent clouds which sometimes penetrate down to the sea surface.

4.2. Heat and moisture fluxes

Due to increasing technical complications the number of so-called "direct" heat flux measurements is smaller than stress observations, and only very few data sets exist for water vapour transports. A good summary of presently available observational results has been published by Friehe and Schmitt (1976). Their graphs form the basis of Figures 5 and 6. Accounting only for data with $|v \cdot (T_a - T_o)| < 30$ [°C m/sec] these authors find that $c_D = 0.91 \cdot 10^{-3}$ (see Figure 5) with insignificant differences for stable and unstable density distribution. Including the high wind speed data of Smith and Banke (1975) c_D assumes a value of $1.41 \cdot 10^{-3}$ (Figure 6). There are still several uncertainties about the sensible heat flux which need to be clarified. The small upward transport at $(T_a - T_o) = 0$ is not yet properly explained and the effect of cold downdrafts due to enhanced cumulus convection has barely been investigated. And a study of the sea spray influences at high wind speeds, which should remarkably affect the surface heat exchange, has just been started by Ling and Kao (1976). At present, errors of the turbulent heat transfer calculations across the air-sea interface of about + 30% may not be very important for models predicting on a time scale of several days but climate studies could presumably suffer much more from this sort of erroneous energy estimates.

Over the ocean, the evaporation of sea water and thus the turbulent moisture flux in the surface layer principally dominates the air-sea energy exchange. And especially over the tropical and subtropical oceans, where the total heat flux into the atmosphere is highest on an annual average, the ratio of $F_0/F_q =$ Bowen ratio is usually less than 0.1 (Hoeber, 1969). Only under cloud cluster conditions is the sensible heat flux found to amount to even more than 25% of the evaporation (Ostapoff et al, 1973). In moderate and higher latitudes, especially in outbreaks of polar air, considerably higher Bowen ratios are to be observed. Unfortunately, not all situations are well documented by direct moisture flux measurements. The few eddy correlation water vapour flux data over oceans are compiled in Figure 7. This is again basically the diagram of Friehe and Schmitt (1976) but some measurements of Kruspe (1976, pers.comm.), which also support the value of $c_q = 1.32 \cdot 10^{-3}$, have been added.

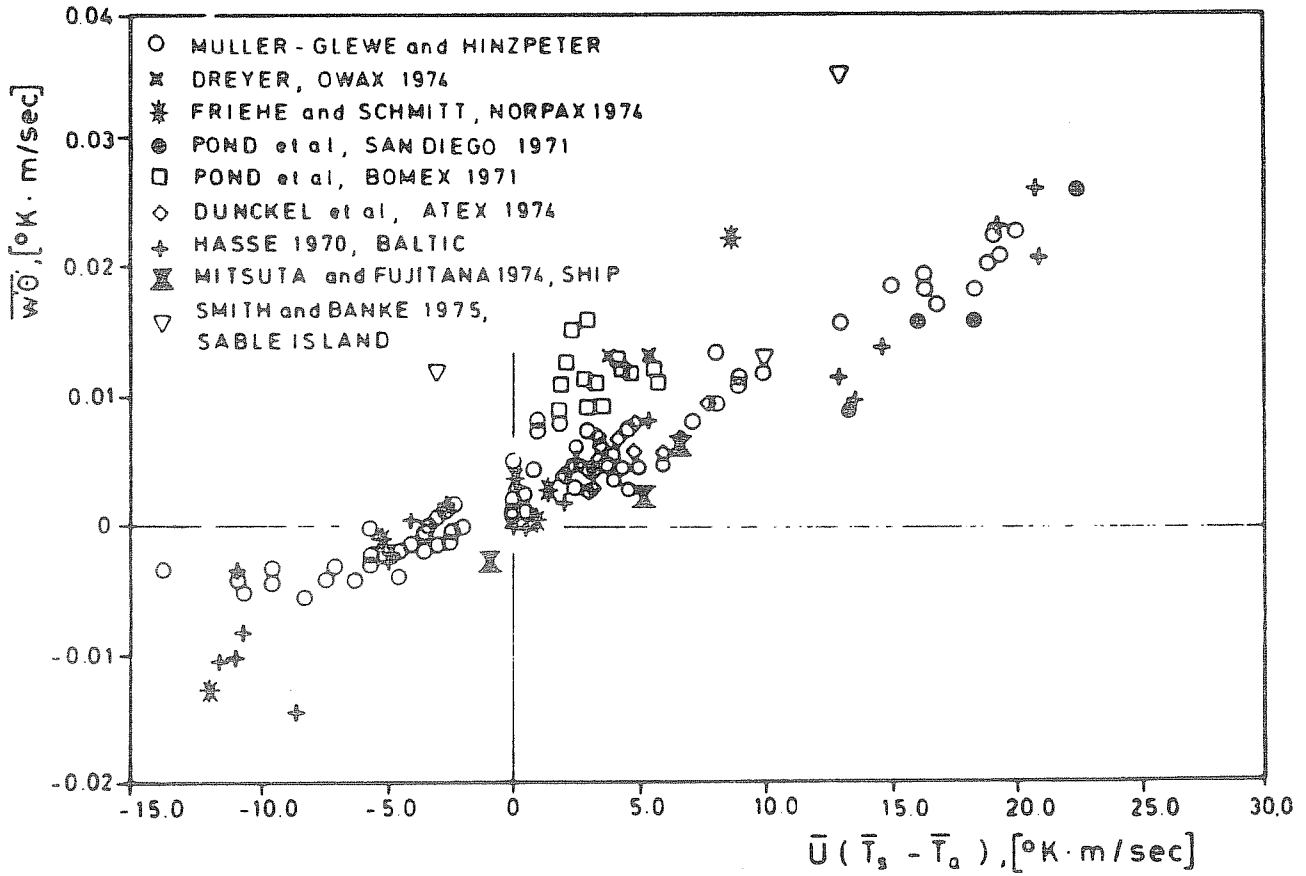


Figure 5. Eddy correlation heat flux versus bulk parameters after Friehe and Schmitt (1976).

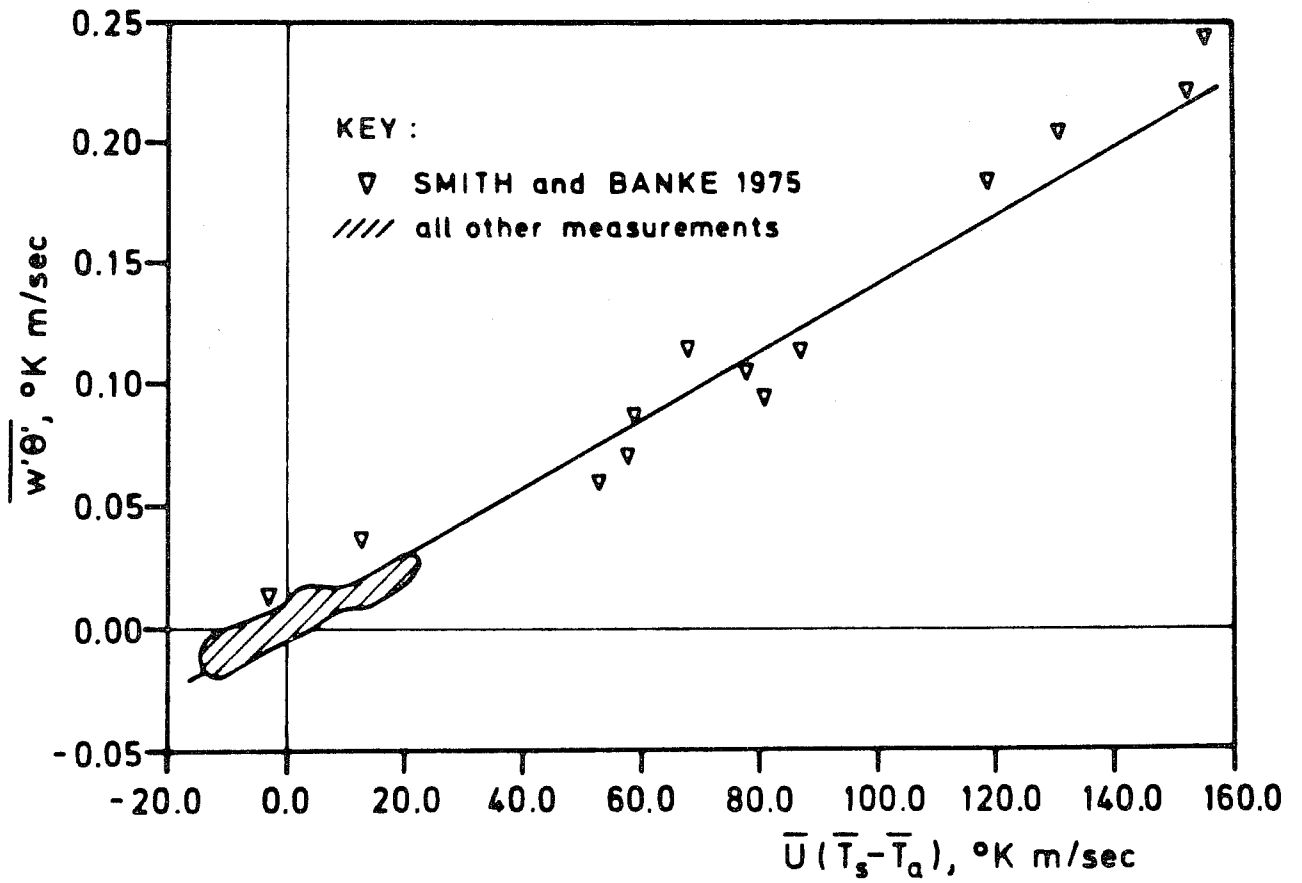


Figure 6. Same as Figure 5 but including the island measurements of Smith and Banke (1975).

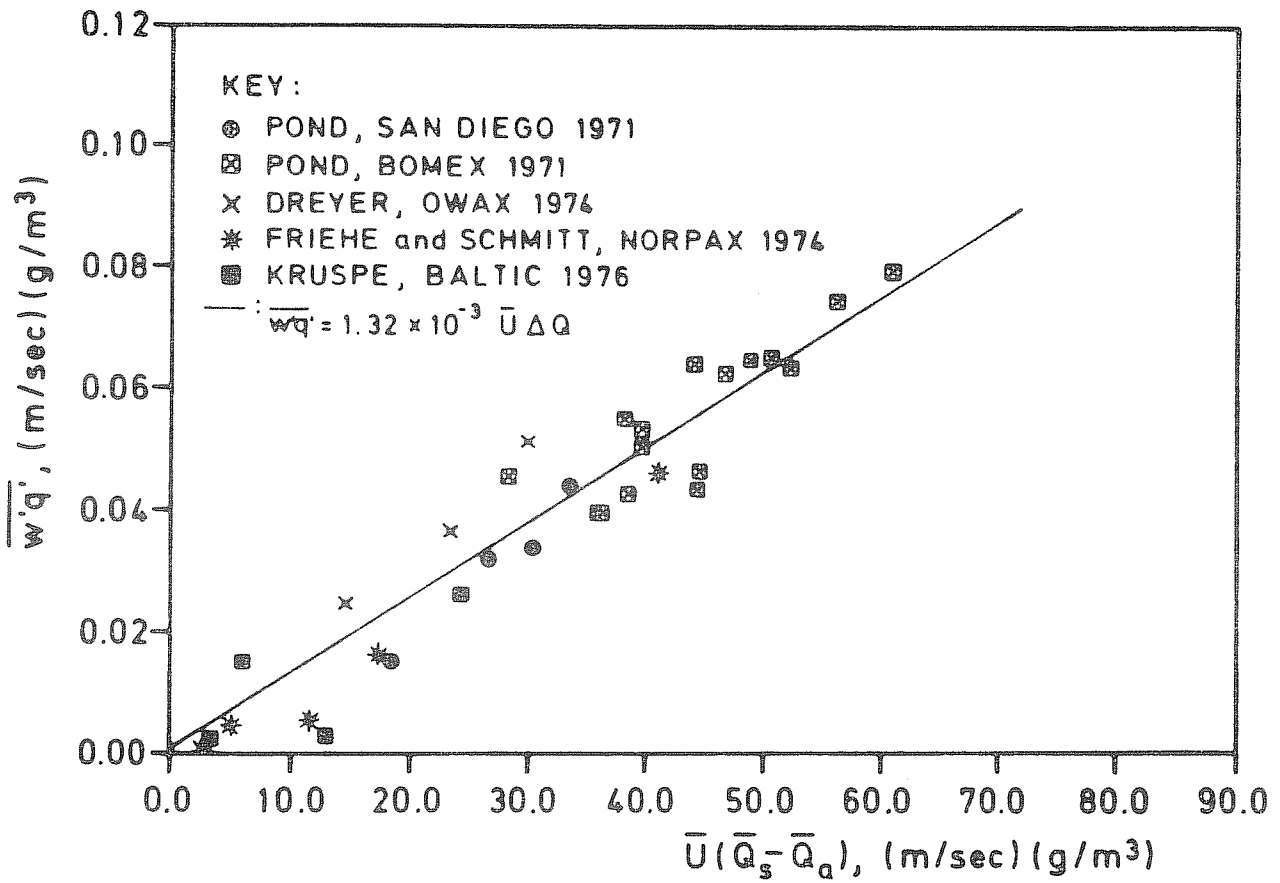


Figure 7. Eddy correlation moisture flux versus bulk parameters after Friehe and Schmitt (1976) and additional data of Kruspe (1976).

Appreciating the technical and natural limitations which have affected the above results, it seems at the moment to be suitable for practical purposes such as application in large scale modelling to assume $c_D=c_0=c_q=1.3 \cdot 10^{-3}$ up to wind speeds of about 15 m/sec. If we allow for an error range of $\pm 30\%$ this value, which corresponds to $z_0=10^{-4}$ meters, agrees with nearly all of the measurements discussed above. Although such a procedure seems to be rather crude, at present there is no known basis for a substantially better approximation. For high wind speeds actual observations do not provide a clear indication as to which kind of parameterization of surface fluxes may be realistic. There is only some indication that an increase of the transfer coefficients with wind speed seems to be probable. Furthermore considerable uncertainty about the flux parameterization exists under pronounced unstationary and inhomogeneous conditions, e.g., during frontal passages.

4.3. Processes at the sea surface

According to laboratory experiments one may assume that at the strong density jump at the sea surface molecular transfer processes would be dominant in the immediate environment of the air-sea interface. As the molecular transfer coefficients for e.g. heat, momentum, and other properties can be determined accurately in the laboratory the transports could be profitably determined from the respective gradients in the conductive region. And in fact Clauss et al (1970) and McAlister and McLeish (1969) were not only able to demonstrate that molecular layers exist in the atmosphere and the ocean, respectively, but they were also able to compute reasonable values for heat fluxes from their data. This method is of course limited to low wind speeds because even slight sea spray effects are sufficient to destroy the ideally sharp air-sea boundary and thus also the pure molecular layers.

With respect to momentum and kinetic energy, in addition to the pure viscous forces (see e.g. Miles, 1957, and Hasselmann et al, 1973) pressure forces acting at the wave perturbations participate in the transfer processes directly at the surface. A proper breakdown of the momentum flux through the sea surface into the viscous stress and into the pressure force could on the one hand help to better specify the frictional resistance of the sea surface to the air flow under various states of the sea. On the other hand good estimates of this ratio are presumably even more important for budgeting the turbulent kinetic energy in the oceanic mixed layer and thus for the determination of the depth of the thermocline.

5. Small scale vertical fluxes above the surface layer

By the term "small scale" we want to cover all wavelengths from the microscale to the largest clouds contributing to the vertical mass, momentum and energy transports. And according to the earlier definition of the ABL these fluxes largely de-

termine its height. Consequently, all of the small scale fluxes generated directly or indirectly at the sea surface should vanish below or at the top of the boundary layer. Unfortunately, over the oceans there are only very few experimental data of the small scale fluxes above the surface layer. At the moment the budget results of ATEX* (Augstein et al, 1973; Augstein and Wagner, 1975, and Brümmer, 1976) and BOMEX** (Holland and Rasmusson, 1973) as well as island observations in the Pacific Ocean (Yanai et al, 1973) form the most comprehensive set of data from the lower troposphere. Additionally, direct aircraft observations have been carried out by Warner (1971), Bean et al (1972), and Pennell and Le Mone (1974). All of these studies have been conducted in lower latitudes and only scarce information is available for moderate and high latitudes. To this author's knowledge simultaneous flux measurements of heat, water vapour, and momentum above the surface layer have only been conducted during the JASIN Project*** near Ocean Weather Ship "J" (Thomson, 1973 and 1974). As there are typical differences between the large scale fields in the Tropics and the Extratropics, e.g., Coriolis-parameter, air mass fronts, baroclinicity, solar radiation, and the structure of tropospheric waves, results obtained at particular latitudes cannot simply be accepted as valid for other regions.

5.1 Momentum transport

Most of the observational momentum flux studies are based on the "ageostrophic" method. In addition to the implication of homogeneity and stationarity of the large scale flow, neither the surface pressure field nor the variation of the pressure gradient force with height (thermal wind) are measured in applying this procedure, but are frequently determined hypothetically. Such approaches might have had their merits in the past as explorative pilot studies but they are insufficient for quantitative investigations of the boundary layer dynamics.

To a good approximation the equations of motion can be written as:

$$\frac{du}{dt} = f(v - v_g) + \frac{1}{\rho} \frac{\partial \tau_x}{\partial z}$$

(7)

$$\frac{dv}{dt} = -f(u - u_g) + \frac{1}{\rho} \frac{\partial \tau_y}{\partial z}$$

* Atlantic Tradewind Experiment, 1969

** Barbados Oceanographic and Meteorological Experiment, 1969

*** Joint Air Sea Interaction Project, 1970

where (u,v) and (u_g,v_g) represent the horizontal components of the actual and geostrophic wind vector, respectively. (τ_x,τ_y) indicate the horizontal stress vector, and ρ and f stand for air density and Coriolis parameter, respectively.

The last terms on the right hand side of Equations (7) can be determined within the ABL if the vertical distribution of (u,v) and (u_g,v_g) and the individual derivatives on the left hand side are observed. Rather often, stationarity and homogeneity are implied, so that the left hand side of Equations (7) becomes zero. And if baroclinicity is considered at all the geostrophic wind is usually assumed to vary linearly with height. The stress profile for an unaccelerated flow is obtained from:

$$\tau_{xz} = \tau_{x0} - \int_0^z f(v-v_g) dz$$

(8)

$$\tau_{yz} = \tau_{y0} + \int_0^z f(u-u_g) dz$$

Equation (8) can be integrated if either the vector $\tau = (\tau_x, \tau_y)$ is known at one certain level or further assumptions like $\tau_{sz} = 0$ where $\partial v_s / \partial z = 0$ are introduced. During BOMEX and ATEX the local time changes as well as the horizontal gradients of the wind components could be estimated. It was found by Holland and Rasmusson (1973) and by Brümmer (1976), respectively that even at 10 degrees latitude these terms are in fact small when averages over several days are considered. The shape of the derived vertical stress profiles of both experiments looked very similar as can be seen from Figure 8. While the BOMEX evaluation is based on the assumption that $\tau_{sz} = 0$ at the lowest height ($\sim 800m$) where $\partial v_s / \partial z = 0$ the ATEX profile has been obtained by starting the integration with the directly observed surface stress τ_0 .

In principle the validity of the first hypotheses is questionable under convective conditions because buoyant air parcels should be able to achieve even counter-gradient fluxes as found for the ATEX τ_s -profile. This speculation is supported by the fact that the BOMEX results arrive at the very low value for c_D of $1 \cdot 10^{-3}$ at the surface. Furthermore, Sutcliffe (1936) applying the same assumption to the observations of the "METEOR" expedition 1925-27, found for c_D a value as small as $0.5 \cdot 10^{-3}$. And with this hypothesis the ATEX data would lead to a c_D of about $0.9 \cdot 10^{-3}$ instead of $1.4 \cdot 10^{-3}$ which has been derived from eddy correlation measurements by Wucknitz (1976). Finally, Pennell and Le Mone (1974) determined remarkable countergradient momentum transports in the upper mixed layer and in the cloud layer from aircraft gust probe measurements over the Caribbean Sea. These results should have a general validity as pure convective influences on the momentum flux should be independent of latitude.

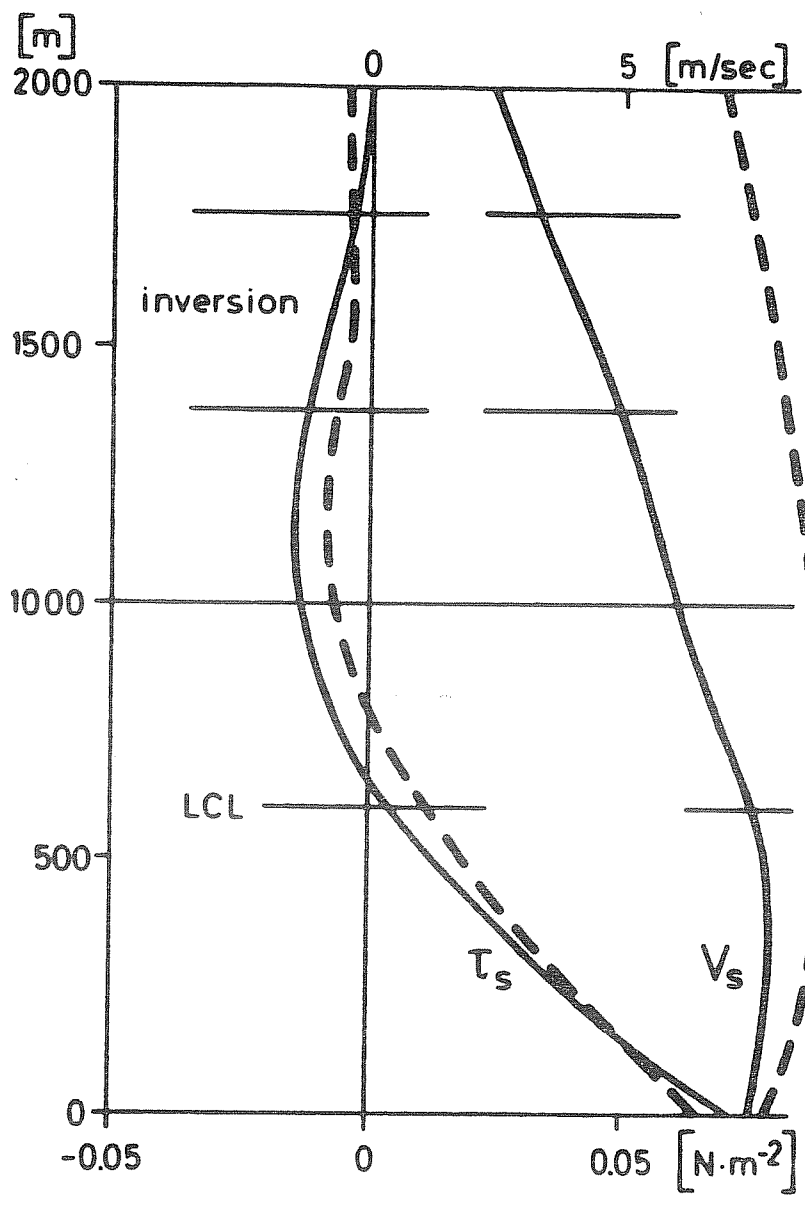


Figure 8. Mean profile of the wind component parallel to the surface wind V_s and the respective stress profile. ATEX full lines, BOMEX dashed lines.

In order to compare the results of various experiments, some characteristic values of the ABL dynamics which have been compiled by Brümmer (1976) are reproduced in Table 1. Except for the BOMEX and ATEX data all the other values come from island observations. Nevertheless, some features which seem to be typical for the trades are expressed similarly in all results. There is only a slight veering of the wind by about 1 degree per 100 m throughout the entire ABL. A weakly pronounced wind maximum lies between 350 m and 800 m height. For application of the resistance law of Kansanskii and Monin (1961) it is interesting to notice that the deviation between the geostrophic and the actual wind at the surface ranges between 13 deg and 26 deg. And with some uncertainty one finds a slight decrease of the angle of ageostrophic air flow with increasing latitude in the Tropics. This tendency is supported by values for $(\alpha - \alpha_g)$ of 11 degrees by Lettau and Hoerber (1964) and of 7 degrees by Augstein and Heinricy (1975) at 55° N. In two case studies in the North Sea, Augstein and Heinricy (1975) have shown furthermore that considerable modifications of the ageostrophic components and of the actual wind profiles (Figure 9) can be caused by horizontal inhomogeneities of the wind field. It was found for a decelerating air stream that the cross isobaric mass flow at the sea surface can even be directed against the pressure gradient for time periods on the order of days (Figure 10). And the cross isobar angle even in moderate zones in accelerated regions obtains a value of 20 deg. Accelerations are of decisive importance at and near the Equator as can be concluded from numerical experiments of Mahrt (1972a and 1972b) and from observations of Estoque (1972). But the presently available observations are hardly sufficient for a proper model verification.

As long as the individual derivatives of the large scale wind components can be determined from measurements or from model computations this effect may be combined with the geostrophic wind to a modified geostrophic wind. Then equations (8) and resistance law approximations can be used in their original form but with the modified values for v_α and $(\alpha_g - \alpha)_0$ as suggested by Hasse (1976).

5.2 Heat and water vapour fluxes

Over the major parts of the oceans the ABL is convectively mixed throughout nearly the whole year. This means that the surface density flux due to heating and moistening from below is directed downwards. Under such conditions the BOMEX and ATEX budget computations lead to sub-grid scale heat and moisture fluxes which coincide in many respects. When the horizontal flow in the ABL is strongly divergent and thus cumulus convection is rather suppressed the small scale heat and moisture fluxes more or less terminate in the inversion layer, as indicated by the solid lines in Figure 11. While water vapour is transported upwards throughout the entire boundary layer sensible heat flux changes its sign below cloud base. Furthermore, it may be noticed that considerable

	Latitude	h_{\max} [m]	$v_{\max} - v_0$ [m/sec]	$\alpha_{500} - \alpha_0$ [deg]	$\alpha_{1000} - \alpha_{500}$ deg	$\alpha_{g_0} - \alpha_0$ [deg]	v_0/v_{g_0}
Christmas Isl. (Estoque, 1971)	2°N	1500	5.6	-6	-9	-	-
ATEX (Brümmer, 1976)	10°N	375	1.1	4	7	26	0.6
BOMEX (Holland and Rasmusson, 1973)	15°N	700	2.2	7	3	21	0.74
ANEGADA (Charnock et al, 1956)	18°N	350	1.2	6	12	13	0.60

Table 1: Height of the wind speed maximum: h_{\max} , wind speed difference between h_{\max} and the surface: $v_{\max} - v_0$, vertical change of wind direction between surface and 500 m height: ($\alpha_{500} - \alpha_0$) and 500 and 1000 m height: ($\alpha_{1000} - \alpha_{500}$), angle of ageostrophic flow at the surface: ($\alpha_{g_0} - \alpha_0$) and the ratio of actual and geostrophic wind speed v_0/v_{g_0} at the sea surface

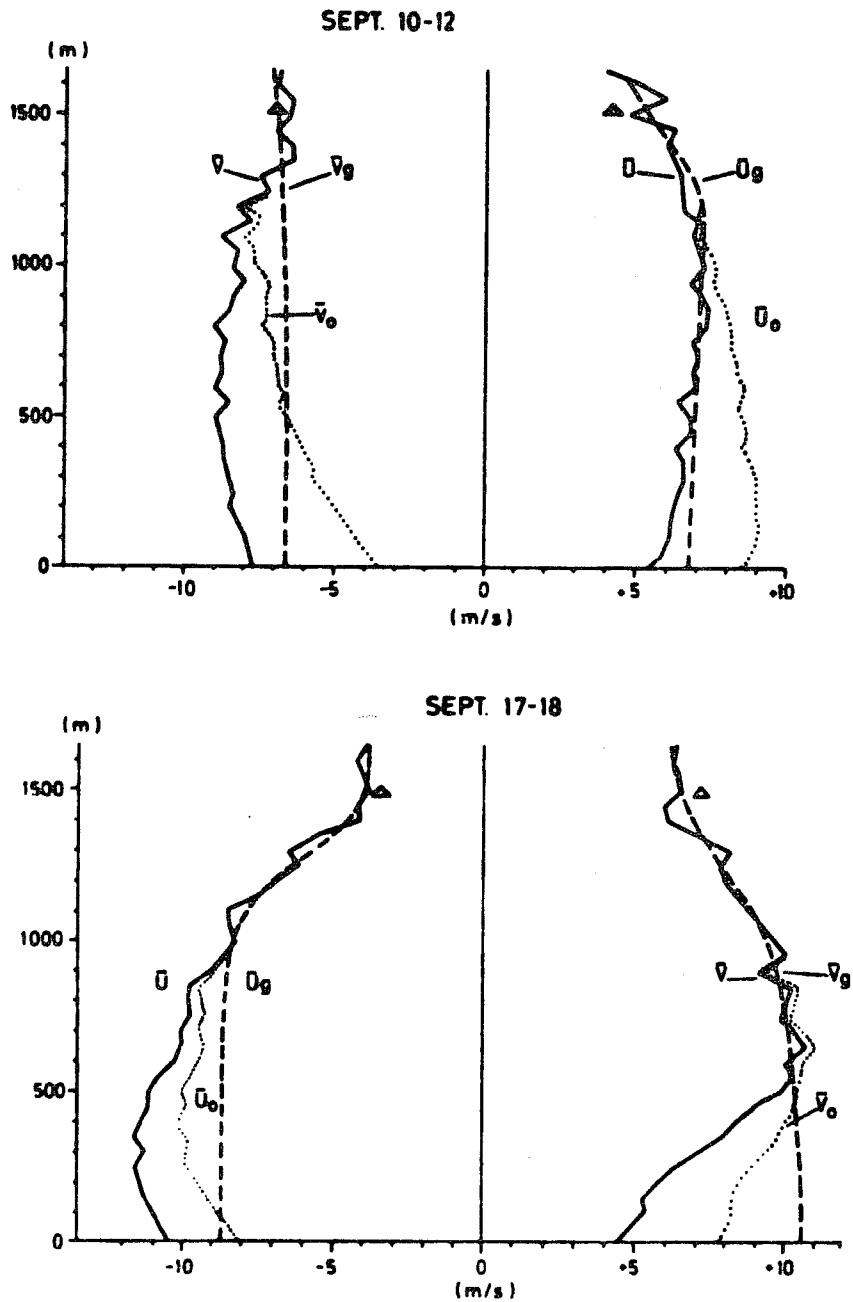


Figure 9. Mean profiles of the zonal and meridional components of the actual (U , V) and geostrophic (U_g , V_g) wind during two periods of JONSWAP II-1973. Dotted lines indicate hypothetical profiles when advective effects are subtracted, after Augstein and Heinrichy (1975).

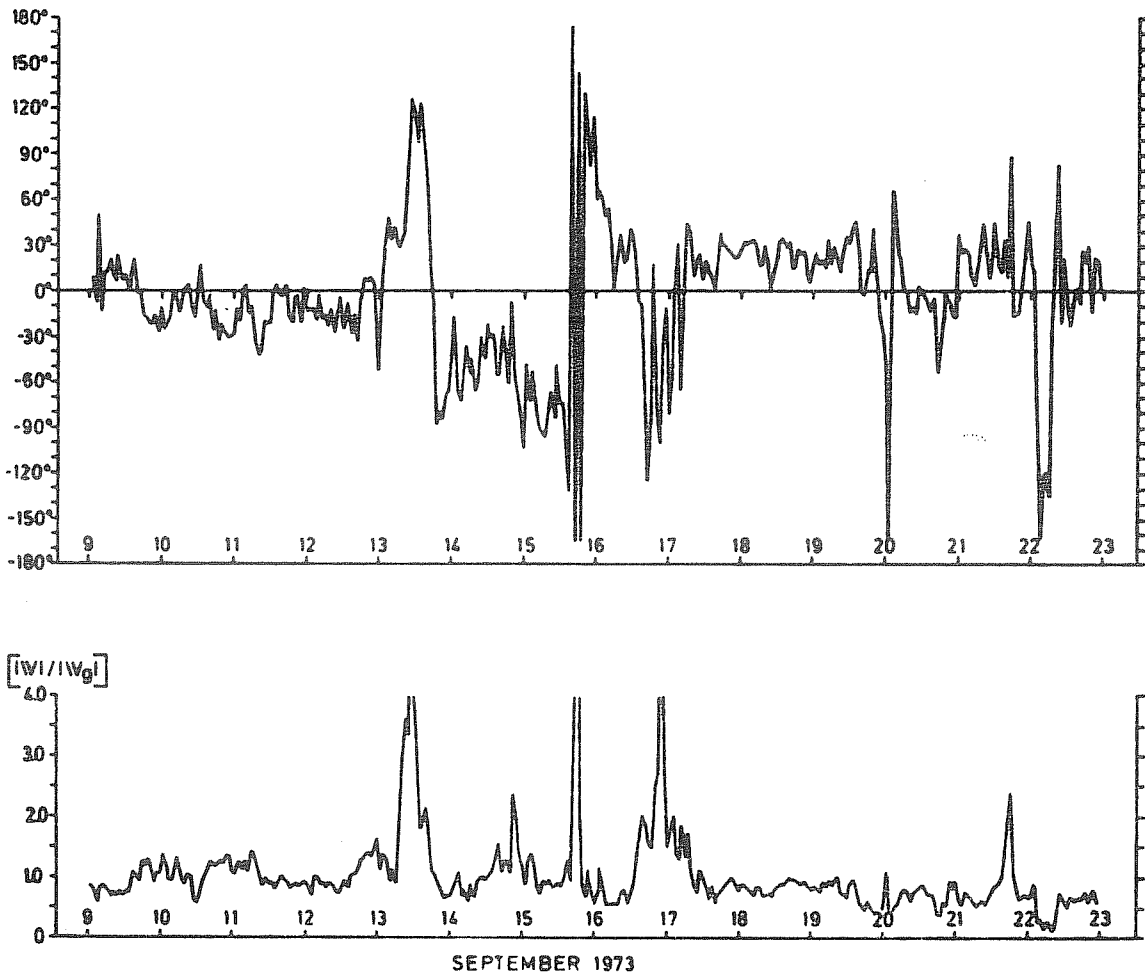


Figure 10. Time series of surface cross-isobar angle ($\alpha_g - \alpha$) above and the ratio of actual to geostrophic surface wind speed (below) during JONSWAP II 1973. After Augstein and Heinricy (1975).

fluxes are observed in particular below cloud base where the vertical gradients of potential temperature and specific humidity vanish. Thus, dry convection must in fact be the major transport mechanism in this region.

In situations with weak low level horizontal divergence or even convergence of the mean flow cumulus convection has been observed to be enhanced. As one consequence the sub-grid scale fluxes reach distinctly higher than the 700 mb level (dash-dotted profiles in Figure 11). And as the trade inversion is simultaneously weak or not present at all no abrupt changes in the flux profiles occur below the 700 mb level. The ATEX data suggest that at least in the Tropics amplified convection seems to be clearly dependent on an increase of water vapour in the lower atmosphere. From these measurements one can conclude furthermore that the enrichment of moisture is not achieved by local evaporation but rather by horizontal advection of water vapour in the lower atmosphere. This fact agrees with practically all measurements in the Hadley regime. They concurrently support the hypothesis that the major part of the water evaporated in the trade wind areas is accumulated in the ABL below the trade inversion and transported downstream into the Inter Tropical Convergence Zone (ITCZ). Here it condensates in deep cumulus clouds and thus generates kinetic energy.

Flux profiles determined as residuals of budget calculations suffer from uncertainties which result from the hypothetical consideration of condensation and evaporation. In the BOMEX and ATEX calculations these effects have been neglected in convectively suppressed conditions and rather crude assumptions have been applied for the convectively active phase. Therefore, other methods are necessary to investigate the processes in detail. Direct measurements of the heat and moisture fluxes by means of tethered balloon sondes will be discussed in the next lecture by Dr. Thompson. Here we will restrict ourselves to some aircraft gust probe results of Warner (1971), Bean et al (1972) and Le Mone and Pennell (1976) which are compiled in Figure 12. Because of technical and statistical sampling problems the observations are mainly concentrated in the subcloud region. Here it can be hoped that the samples provide a representative area mean because enough elements of the effective wavenumbers can be sensed during an aircraft run. In the cloud layer vertical mixing is mainly carried out by a small number of clouds the updrafts of which may cover only about 5% of the horizontal plane. Therefore it is a complicated task to collect a statistically significant number of events over a certain area during a reasonable time interval. Fair weather flights show the same features for the subcloud layer as the budget results. Hopefully some flights during GATE* will also offer some quantitative values of disturbed situations. Heat and moisture fluxes in the upper ABL over the oceans in higher

*GATE: GARP Atlantic Tropical Experiment

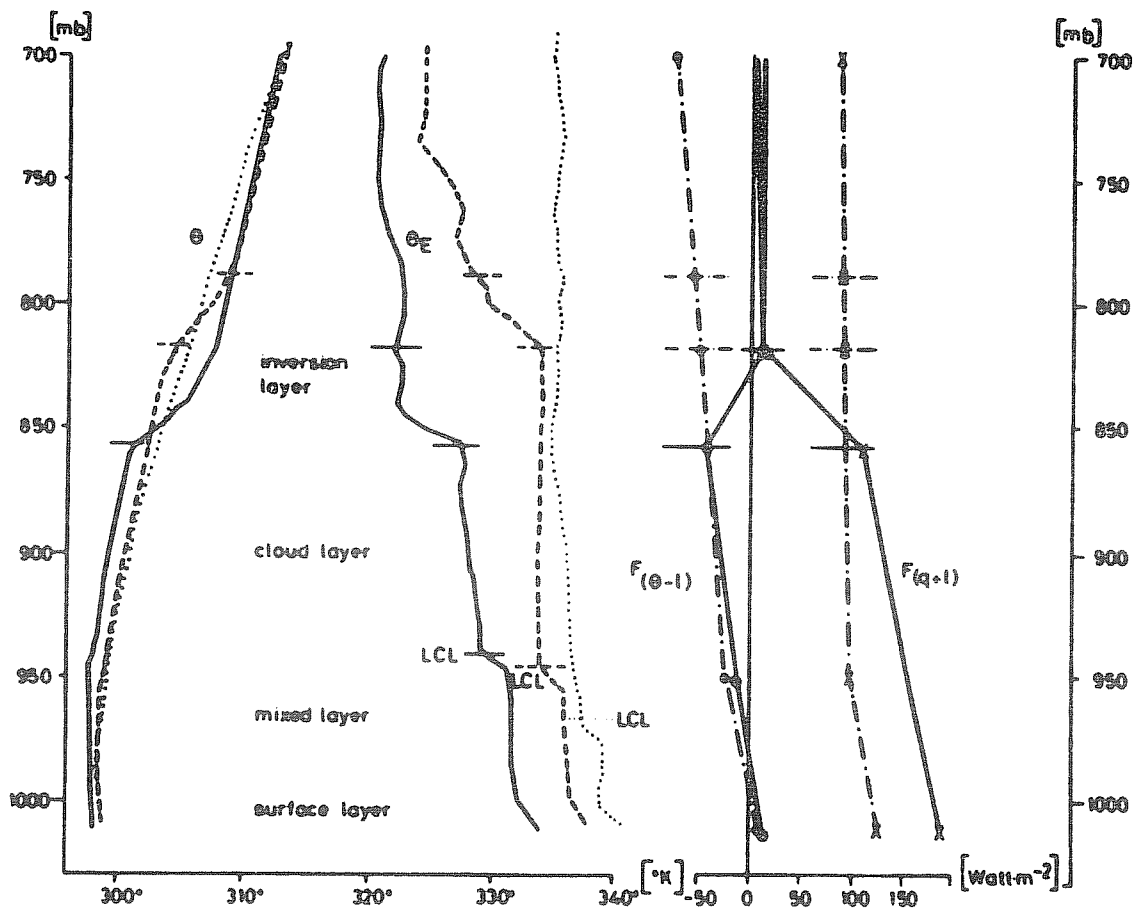


Figure 11. Mean ATEX profiles of potential temperature Θ , equivalent potential temperature Θ_E , heat flux $F_{(\Theta-1)}$ and water mass flux $F_{(q+1)}$. Condensation and evaporation are not accounted for. Full lines : undisturbed trade wind conditions. Broken and dotted profiles: disturbed conditions with (dashed) and without inversion present. Dash-dotted lines represent fluxes in disturbed conditions. LCL = lifting condensation level of surface air.

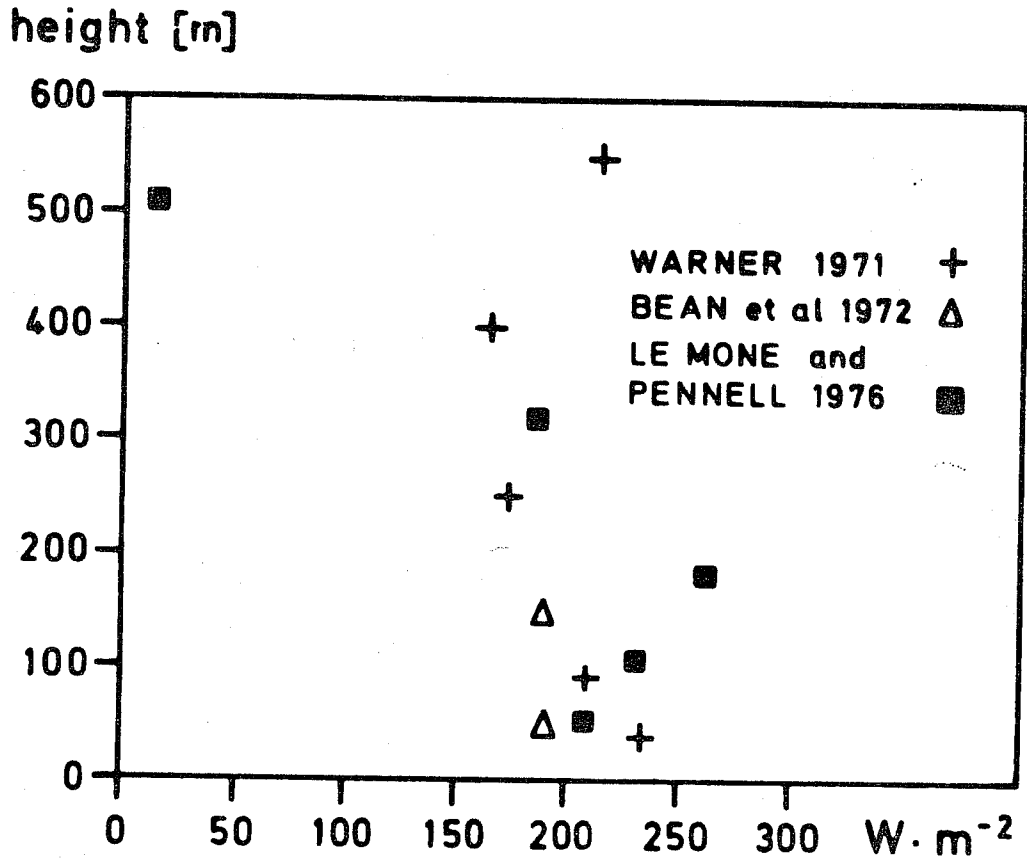


Figure 12. Flux of moist static energy $h = cpT + gz + Lq$ measured by air craft gust probes by Warner (1971), Bean et al (1972) and Le Mone and Pennell (1976).

latitudes are for all practical purposes not available in the literature. Tethered balloon measurements during ATEX and past JASIN experiments are discussed only in some internal Technical Reports and they are regarded by the authors much more as instrumental tests rather than proven results.

All the measurements presented so far cover situations with cumulus clouds participating in the boundary layer transports. Fluxes within the simpler pure mixed layer with or without stratiform clouds in its top region have not yet been measured over the ocean. In this case not only flux measurements but also radiation studies would be of great importance.

From the results just discussed the following conclusions may be drawn about the small scale fluxes within convective boundary layers:

- a) The heat flux is upwards in the major part of the subcloud layer and downwards in the cloud layer with a maximum value at the base of the capping inversion.
- b) The moisture flux is upwards from the sea surface to the inversion layer. It decreases slightly with height up to the inversion base and converges rapidly in the inversion layer.
- c) Heat and moisture fluxes more or less terminate in the inversion region if only small clouds exist.
- d) Together with enhanced cloudiness the small scale transports penetrate the inversion or destroy it totally. They proceed upwards into the middle or even high troposphere.
- e) The effect of air mass fronts in moderate latitudes on vertical exchange processes has not yet been treated observationally in desired detail.

6. The layered structure of the ABL

The mean vertical static, thermodynamic and kinematic structures of the ABL may be regarded as statistical parameters which are composed as a net effect of a number of processes acting on the atmospheric air particles. Although the relationship between the mean profiles and the combination of processes is not unique, prognostic modelling is possible if the initial state is known and the acting processes can be satisfactorily simulated. In order to fulfill the latter requirement one tries to express small scale events by mean (grid scale) parameters. And in addition to investigating the ABL physics "per se" it is particularly this so called parameterization task which stimulates the actual observational research. Progress in this field is based on a sufficient knowledge of the scale interaction within the spectrum of atmospheric motion as well as the influences of radiation, condensation, droplet evaporation, rainfall, etc. In addition to the mean motions and stochastic turbulence, perturbations which are organized into so called secondary flow patterns can be very important in the ABL transport processes. These phenomena cannot be treated successfully within the frame of Reynolds turbulence but other mechanisms like Rayleigh instability (buoyancy exceeds molecular and microscale

turbulence forces) and inflection point instability (due to angular momentum transfer when the vertical wind profile has an inflection point) are to be considered. In this area field observations are lagging behind the actual model concepts, the improvement of which needs experimental guidance.

In agreement with observations and model results we may roughly distinguish between three types of ABLs:

- a) a pure mixed layer capped by a strong temperature inversion,
- b) a mixed-cloud layer structure also capped by a temperature inversion and
- c) a mixed-cloud layer version with deep clouds and no clearly defined upper boundary.

Subsequently we will try to shed some light on the physical background of the development of these different structures.

6.1. Weakly disturbed conditions

By 'weakly disturbed' we characterize large scale conditions which allow no cloud formation or the development of small non-precipitating cumuli in the lower atmosphere. Such situations are typical for the major part of the trade wind flow but they are also observed in higher latitudes in subsiding air of high pressure cells. In regions of cold coastal upwelling along the west coasts of the subtropical continents the ABL consists simply of a shallow mixed layer as shown in Figure 13. There is only a relatively small upward moisture flux at the sea surface and the sensible heat flux can even be directed into the ocean. Consequently, the small scale entrainment forces are already balanced by the subsidence at a low level. The mixed layer characteristics remain unchanged even when the inversion is pushed somewhat beyond the condensation level and stratiform clouds develop. But then radiative cooling at the cloud tops effectively contributes to the generation of turbulent kinetic energy. And as Lilly (1968) and recently Deardorff (1976) have demonstrated upward mixing is amplified. This effect may destabilize the stratus layer and lead to cumulus development. A cumulus layer is generally observed further downstream where the upward surface fluxes increase and the large scale subsidence gradually decreases. In this part of the trades the second type of ABL develops which is represented by the full profiles in Figure 14.

Due to condensational heating the buoyancy of the saturated ascending air parcels is enhanced. And consequently, further small scale kinetic energy is generated. A part of it is converted into potential energy when the cloud tops overshoot their level of static equilibrium.

Due to the combination of processes the ABL is now composed of 5 sublayers. While the inversion at the top is principally ge-

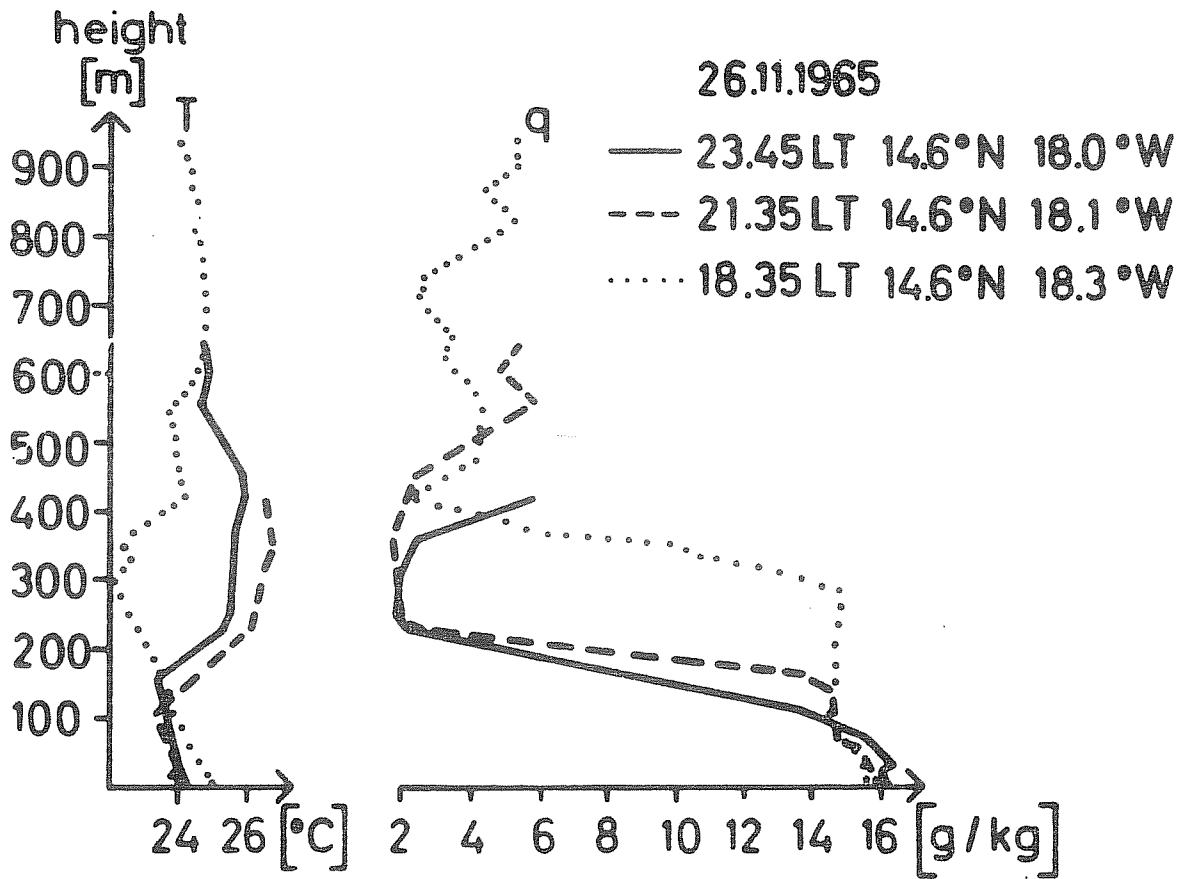


Figure 13. Vertical profiles of temperature (T) and specific humidity (q) near the African west coast. Measured during a "Meteor" cruise 1965.

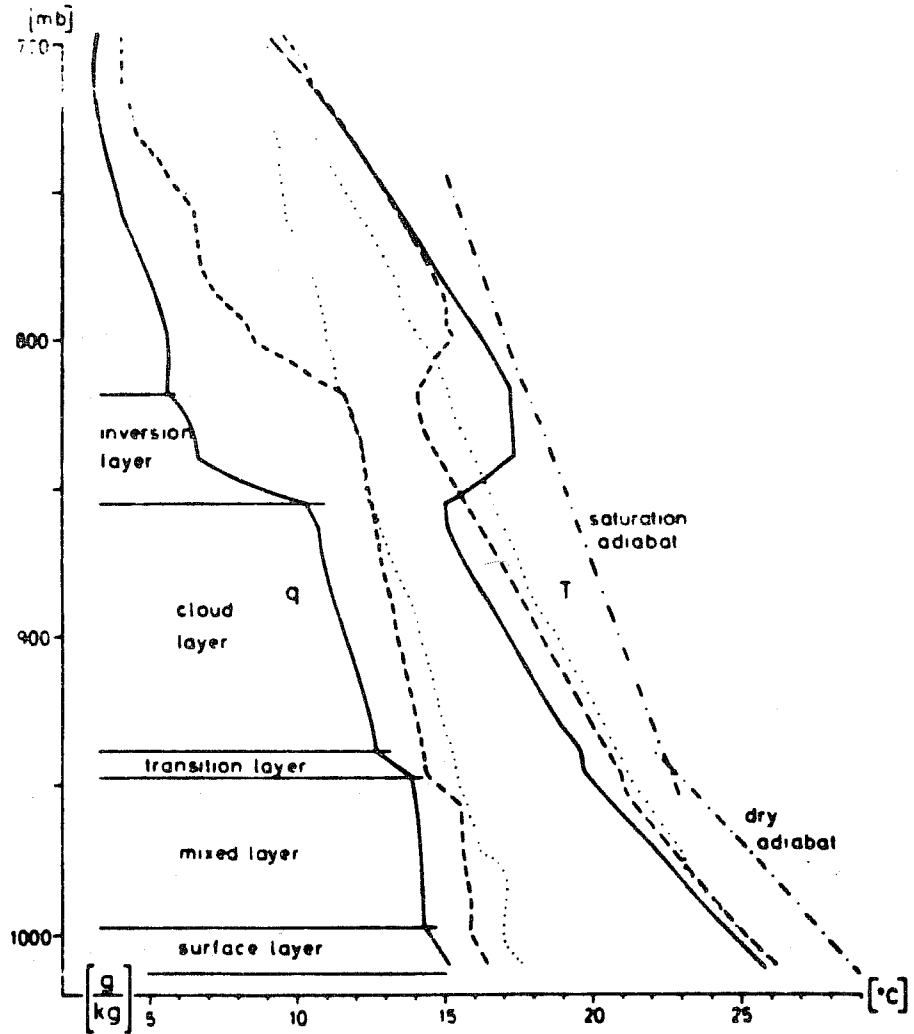


Figure 14. Vertical distribution of temperature (T) and specific humidity (q) in undisturbed trades (full lines), in slightly (dashed) and strongly (dotted) disturbed situations.

nerated and maintained in the same way as the capping inversion of the mixed layer the stable transition region between the mixed and cloud layer still needs to be explained. Measurements of Holland (1975) and of Le Mone and Pennell (1976) in Figure 15 document that the updrafts of trade wind cumuli originate below the condensation level at some height within the mixed layer. Therefore, the compensating downward mass flux in the cloud free environment adds to the large scale subsidence. And a stable layer forms where the combined downward motion is balanced by upward mixing due to mechanical turbulence and dry convection. Only the very powerful buoyant elements are able to penetrate to their condensation level and to form new clouds. Directly below active clouds in the updraft areas the transition layer is in fact not present (Holland, 1975). In general increased cloudiness will amplify subsidence in the cloud free regions and thus force the transition layer downwards. In reaction cloud development will be reduced. The transition layer in turn will be able to migrate upwards and the opportunity for cloud formation becomes more favourable again. From this circle of processes one should expect a close interrelation between cumulus activity and the height of the transition layer. During ATEX, a significant correlation between the daily means of the lifting condensation level (LCL) of surface air and the height of the transition layer became in fact obvious, as documented in Figure 16. Similar conclusions about the interaction between the cloud and the subcloud layer on the basis of BOMEX-data have been drawn by Sarachik (1974) and Esbensen (1975).

Further insight into the interaction between the various boundary layer processes can be gained from the diurnal variations of the several quantities displayed in Figure 17. The vertical entrainment velocity w_e at the inversion base, which has been determined as a residual of the large scale mass transports and the height variation of the inversion is assumed to be a good indicator for cloud activity. As the large scale subsidence turned out not to vary diurnally, short wave radiation is left as the main basic trigger mechanism for the observed changes. In accordance with model computations of Hinzpeter (1968) the derived amplitude of the diurnal temperature wave increases with height from the sea surface up to the trade inversion. Its phase relation coincides with that of the air-sea temperature difference in Figure 17. Thus, static stability has a minimum in the early morning and a maximum in the afternoon. This obviously leads to the variation of cloudiness as represented by w_e . During the period of increased convective activity (big arrow) the transition layer has its minimum height while the trade inversion is forced upward. When convection is less pronounced (small arrow) the transition layer has its maximum height and the inversion migrates downward. With respect to the energy exchange at the sea surface, the sensible heat flux is modified by

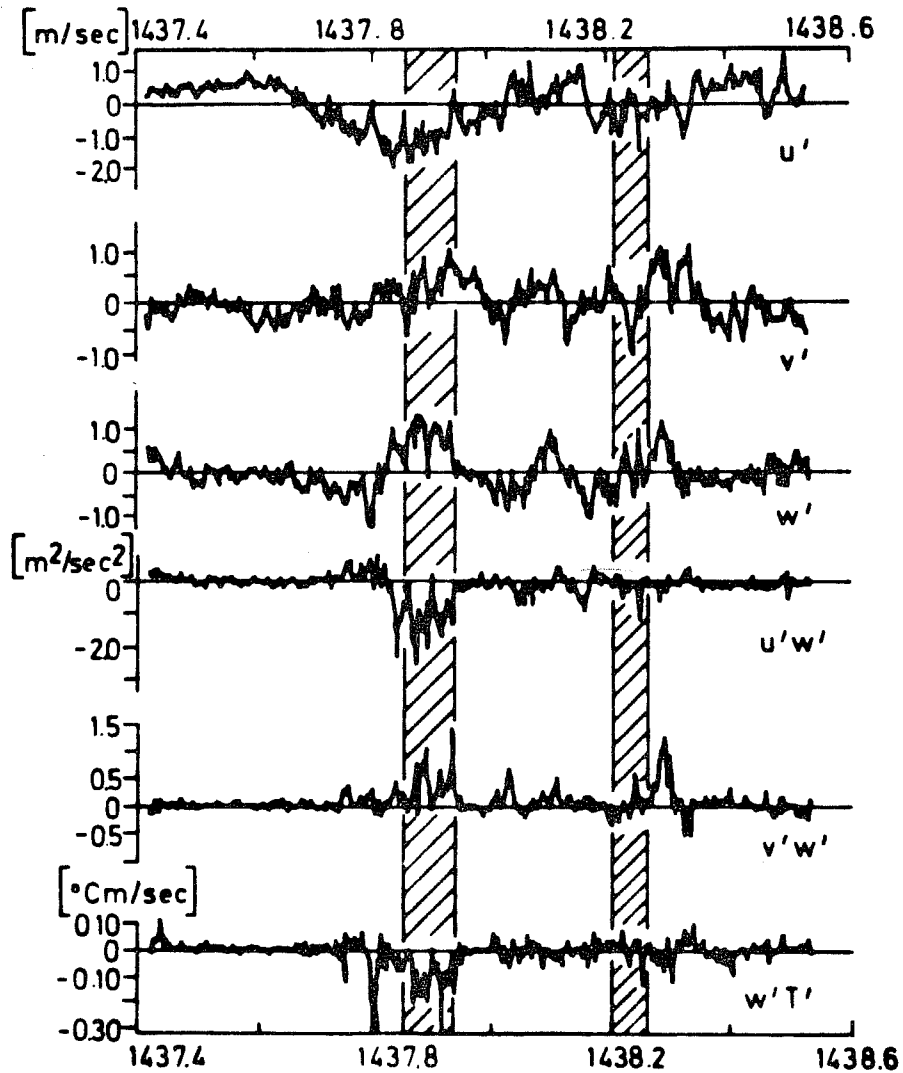


Figure 15. Gust probe measurements below cloud base near the Caribbean by Le Mone and Pennell (1976) Shaded areas are below clouds.

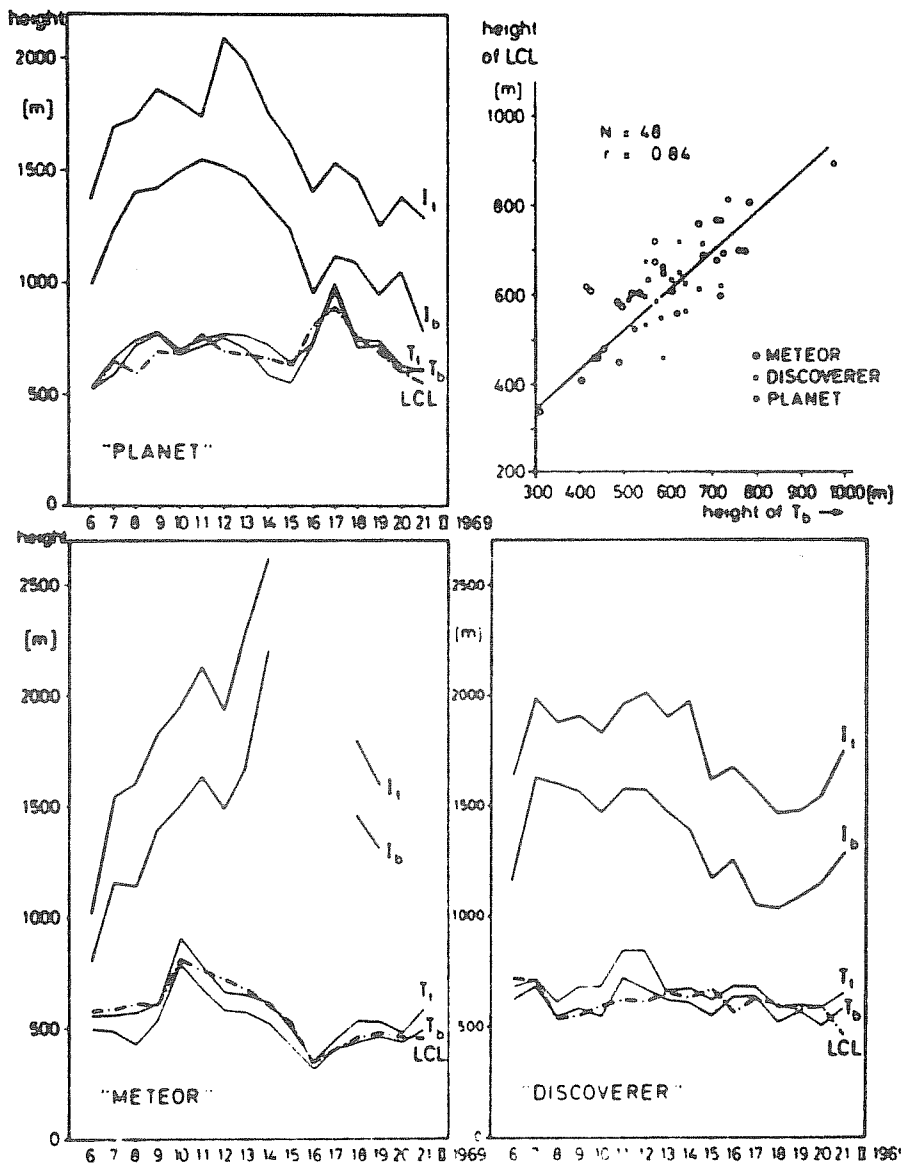


Figure 16. Time series of daily averages of inversion base (I_b) and inversion top (I_t), transition layer base (T_b) and transition layer top (T_t) as well as the lifting condensation level (dash-dotted) of surface air at the ATEX ships.

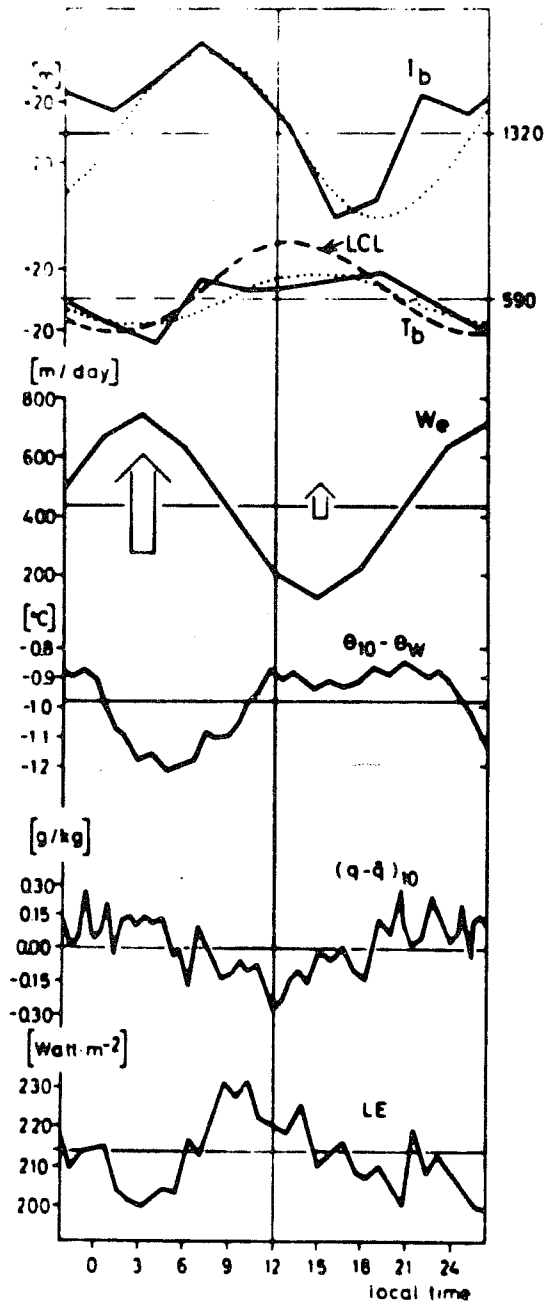


Figure 17. Diurnal variation of the inversion base I_b , the base of the transition layer T_b , the lifting condensation level LCL, the entrainment velocity at the inversion base W_e , the air-sea temperature difference $\theta_{10} - \theta_w$, the difference between the actual specific humidity q and the daily average q at 10 m height and the surface evaporation LE.

the diurnal cycle of short wave absorption in the air and it could directly amplify the 24-hourly convective mode. In contrast to the sensible heat flux evaporation does not force the variation of cloudiness; it rather reacts upon changes of convective activity. In consistence with the earlier conclusions about the mass flux at cloud base level we find that enhanced convection decreases the moisture content^o of the mixed layer as indicated in Figure 17 by the specific humidity variations at 10 m height. This drying effect causes an upward displacement of the LCL (negative feed back on convection) and an increase of evaporation at the sea surface (positive feed back on convection). Unfortunately, the insufficient humidity measurements obtained from the radiosondes during ATEX (see: Ostapoff et al, 1970) do not permit an exact quantitative investigation of the variation of the moisture fluxes at cloud base. But if we assume that the moisture variation throughout the mixed layer is the same as that near the sea surface - where it should have a minimum value - the convective water vapour flux at cloud base would diurnally vary by about 30%. These examples suggest a very sensitive balance between the various processes in the atmospheric boundary layer, the exchange mechanisms at the air-sea interface and the thermal and kinematic characteristics of the large scale field even in a rather uniform air flow.

6.2. Strongly disturbed conditions

Strong amplification of convective perturbations generally requires horizontal convergence of the low level atmospheric flow in order to achieve the necessary water vapour supply at cloud base. This fact is also included in the CISK*-hypothesis of Charney and Eliassen (1964) and Ooyama (1964). In moderate zones of the Earth other large scale forcing mechanisms are also important, e.g. warm and moist air overriding the underlying cold air at warm fronts and destabilization of cold polar air over warm water surfaces by heating and moistening from below. Satellite photographs show in such cases rather frequently the presence of cloud streets and three dimensional open or closed convective cells. First attempts to explain these features by the thermodynamic Rayleigh mechanism by Krishnamurti (1975) are very promising. Although the air-sea energy exchange under large precipitating clouds can be strongly modified and the Bowen ratio may vary between 0.05 and 0.3 (Ostapoff et al, 1973), according to Reed and Recker (1971) the horizontal water vapour advection still seems to be a decisive prerequisite for deep cloud development. On the other hand, Sequin and Garstang (1976) have provided evidence that intense convection significantly modifies the mixed layer. They have pointed out that in such situations the static stability is increased while the moisture content is reduced in the sub cloud layer. Preliminary GATE results of Emmitt (1976) clearly document that the undrafts

*CISK: Conditional Instability of the Second Kind

of enhanced tropical cumuli originate in the lower part of the mixed layer (Figure 18). And cold downdrafts, as described by Zipser (1969), contribute remarkably to the interaction between the cloud and the subcloud layer. That these motions penetrate right down to the sea surface is well reflected in the temperature, humidity, and wind velocity records of the 'METEOR' buoy during GATE in Figure 19. Comparing the temperature profiles before and after the passage of a disturbance in Figure 20, two facts are remarkable. Firstly, the mixed layer height is much lower to the rear of the storm and secondly, the air is cooled in the lowest 1500 m of the atmosphere. Concluding from the equivalent potential temperature (Figure 21), this air seems to originate from the cloud layer above 2000 m height ahead of the disturbance as predicted e.g. by the cloud model of Moncrieff and Miller (1976).

At present, our knowledge about the behavior of the ABL in disturbed situations is mostly of a qualitative nature. Presumably GATE will narrow this knowledge gap to some extent for the Tropics. Further experimental efforts are nevertheless necessary in order to study the various disturbed cases in moderate and high latitudes. These data could then provide a satisfactory observational background for theoretical investigations and modelling purposes.

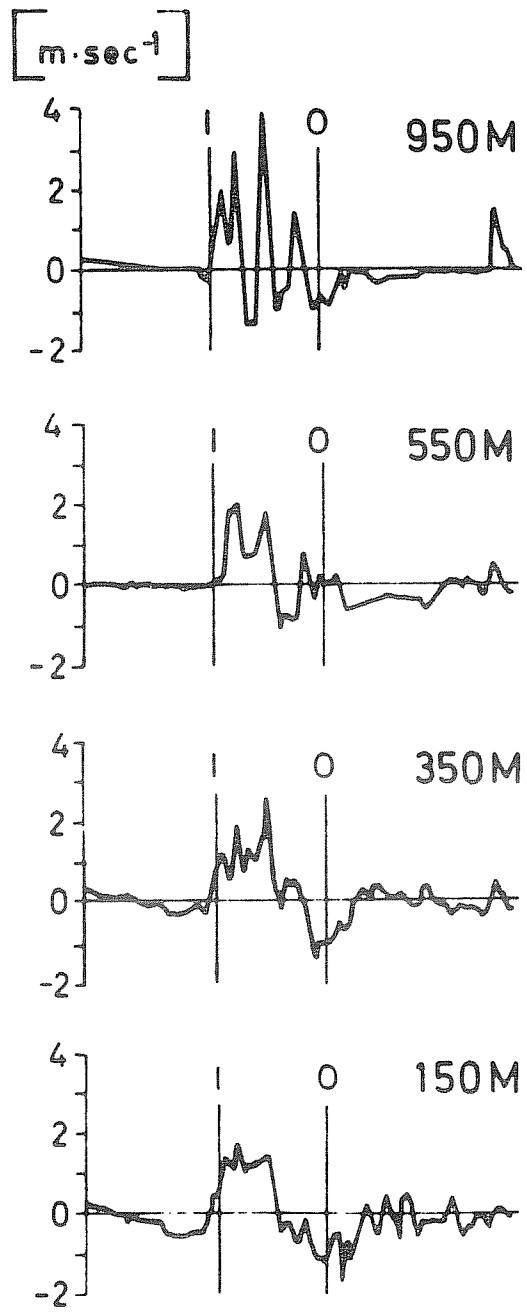


Figure 18. Vertical motion during a cloud passage (from I to O) measured at a tethered balloon simultaneously at 4 heights during GATE. After Emmitt (1976).

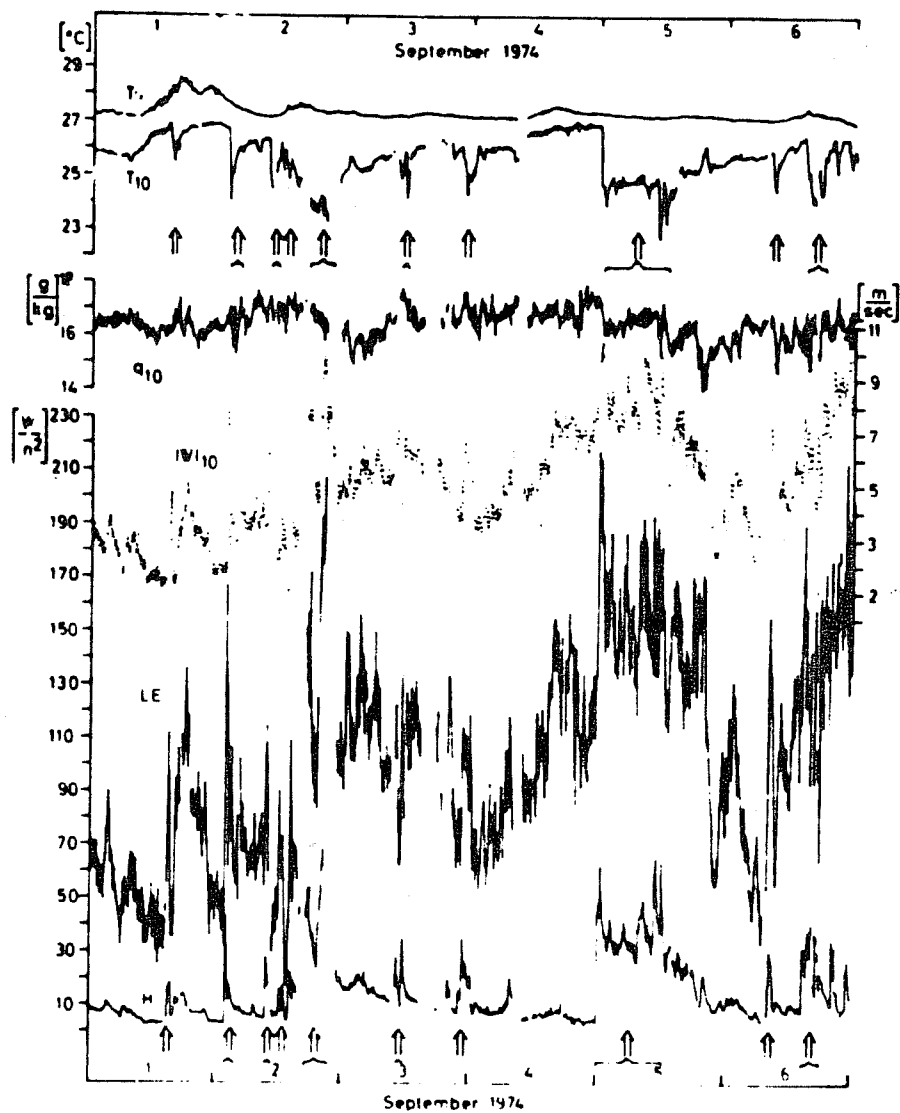


Figure 19. Buoy measurements during GATE at R.V. "Metcor". T_s = sea surface temperature; T_{10} = air temperature, q_{10} = specific humidity, $|W|_{10}$ = wind speed at 10 m height; LE = evaporation, H = sensible heat flux. Big arrows indicate rainfall periods.

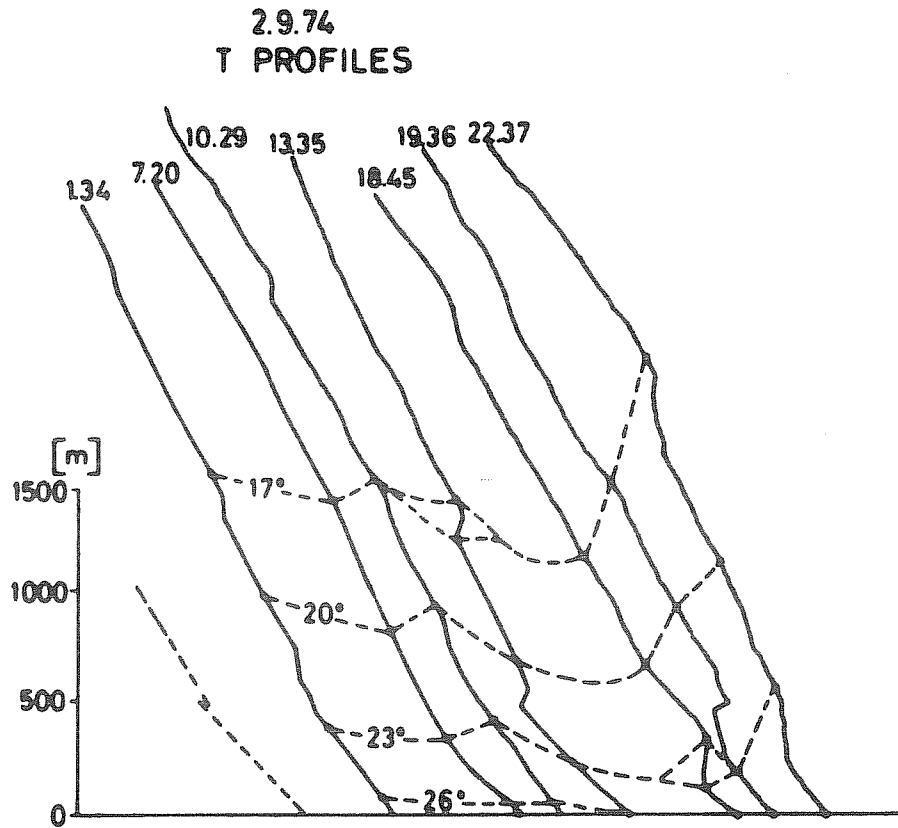


Figure 20. Temperature profiles before (1.34, 7.20, 10.29), during (13.35) and after (18.45, 19.36, 22.37) the passage of a disturbance during GATE at the R.V. "Fay".

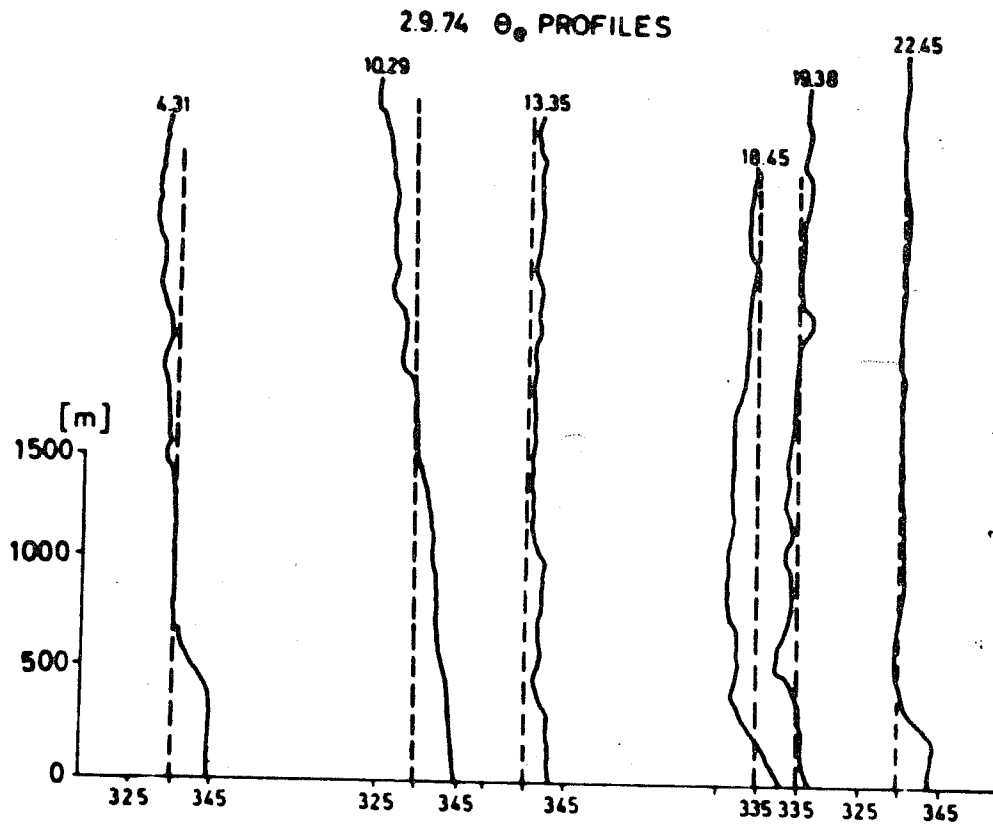


Figure 21. Same as Figure 20, but equivalent potential temperature.

7. References

- McAlister, E.D., and McLeish, W. (1969): Heat transfer in the top millimeter of the ocean. *J. Geoph. Res.* 74, 3408-3414
- Arakawa, A., and Schubert, W. (1974): Interaction of a cumulus cloud ensemble with the large scale environment. Part. I. *J. Atm. Sciences* 31, 674-701
- Augstein, E., Riehl, H., Ostapoff, F., Wagner, V. (1973): Mass and energy transports in an undisturbed Atlantic trade wind flow. *Month. Weath. Rev.* 101, 101-111
- Augstein, E., and Wagner, V. (1975): Vertical coupling within the Hadley circulation over the Atlantic Ocean. *Beitr. Phys. Atm.* 48, 103-118
- Augstein, E., and Heinrich, D. (1975): Actual and geostrophic wind relationships in an accelerated marine atmospheric boundary layer. *Beitr. Phys. Atm.* 49, 55-68
- Badgley, F.I., Paulson, C.A., and Miyake, M. (1972): Profiles of wind, temperature and humidity over the Arabian Sea. *Meteor. Monogr.* 6
- Ball, F.K. (1960): Control of inversion height by surface heating. *Quart. J. Roy. Met. Soc.* 86, 483-490
- Bean, B.R., Gillmer, R., Grossman, R., McGarvin, R. Travis, T. (1972): An analysis of airborne measurements of vertical water vapour flux during BOMEX. *J. Atm. Sciences* 29, 860-869
- Betts, A.K. (1973): Non-precipitating cumulus convection and its parameterization. *Quart. J. Roy. Met. Soc.* 99, 178-196
- Brocks, K., and Krügermeyer, L. (1972): The hydrodynamic roughness of the sea surface. *Stud. Phys. Oceanogr.* I, 75-92
- Brümmer, B. (1976): The kinematics, dynamics and kinetic energy budget of the trade wind flow over the Atlantic Ocean. *Meteor-Forsch. Erg.* B 11 (in print)
- Carson, D.J. (1973): The development of a dry inversion-capped convective unstable boundary layer. *Quart. J. Roy. Met. Soc.* 93, 450-467
- Charnock, H., Francis, J.R.D., and Sheppard, P.A. (1956): An investigation of wind structure in the trades. *Phil. Trans. Roy. Soc. London, Series A* 249, 179-234
- Clauss, E., Hinzpeter, H., Müller-Glewe, J. (1970): Ergebnisse von Messungen des Temperaturprofils der Atmosphäre nahe der Grenzfläche Ozean-Atmosphäre. *Meteor. Forsch. Erg.* B 5, 85-89

- Deardorff, J.W. (1972): Numerical investigation of neutral and unstable planetary boundary layers. *J. Atm. Sciences* 29, 91-115
- Deardorff, J.W. (1976): On the entrainment rate of a stratocumulus-topped mixed layer. *Quart. J. Roy. Met. Soc.* 102, 563-582
- Emmitt, C.D. (1976): Cumulus structure from near cloud base to the surface (in preparation)
- Esbensen, S. (1975): An analysis of subcloud layer heat and moisture budgets in the western Atlantic trades. *J. A. S.* 32, 1921-1933
- Estoque, M.A. (1971): The planetary boundary layer over Christmas Island. *Month. Weath. Rev.* 99, 193-201
- Friehe, C.A., and Schmitt, K.F. (1976): Parameterizations of air-sea interface fluxes of sensible heat and moisture by the bulk aerodynamic formulas. (to be published in *J. Phys. Oceanogr.*)
- Garratt, J.R., and Hyson, P. (1975): Vertical fluxes of momentum, sensible heat and water vapour during the Air Mass Transformation Experiment (AMTEX) 1974. *J. Met. Soc. Jap.* 53, Nr. 2, 149-160
- Hasse, L. (1968): On the determination of the vertical transports of momentum and heat in the atmospheric boundary layer at sea. *Hamb. Geoph. Einzelschr.* H. 11, 70pp
- Hasse, L. (1976): A resistance-law hypothesis for the instantaneous advective planetary boundary layer. *Bound. Layer Met.* 10 (in print)
- Hasselmann, K. and 15 co-authors (1973): Measurement of wind-wave growth and swell decay during the Joint North Sea Wave Project. *DHZ, Reihe A*, Nr. 12
- Hinzpeter, H. (1968): Tagesperiodische Änderungen des oberflächennahen Temperaturfeldes über dem Meer als Folge von Strahlungsquellen und -senken. *Kieler Meeresforsch.* 24, 1-13
- Hoeber, H. (1969): Wind-, Temperatur-, Feuchteprofile in der wassernahen Luftschicht über dem äquatorialen Atlantik. *Meteor-Forsch. Ergeb.* B 3, 1-26
- Holland, J.Z. (1975): Characteristics of the lower atmosphere near Saipan, April 29 to May 16, 1945. *NOAA Techn. Mem. EDS CEDDA-2*, 20 pp
- Holland, J.Z., and Rasmusson, E.M. (1973): Measurements of atmospheric mass, energy and momentum budgets over a 500-km square of tropical ocean. *Month. Weath. Rev.* 101, 11-55

- Kasanskii, A.B., and Monin A.S. (1961): On the dynamical interaction between the atmosphere and the Earth's surface. Izv. Akad.Nauk, Ser.Geof.5
- Kitaigorodsky, S.A. (1970): The physics of air-sea interaction. Gidrometeorologicheskve Izdatel'stvo, Leningrad 1970
- Krishnamurti, R. (1975): On cellular cloud patterns. Part 1, Part 2, Part 3. J.A.S.32, 1354-1383
- Kruspe, G. (1976): personal communication.
- De Leonibus, P.S. (1971): Momentum, flux and wave spectra observations from an ocean tower. J.Geoph.Res. 76, 6506-6527.
- Lettau, H.H., and Hoerber H. (1964): Über die Bestimmung der Höhenverteilung von Schubspannung und Austauschkoefizient in der atmosphärischen Reibungsschicht. Beitr. Phys. Atm. 37, 105-118
- Lilly, D.K. (1968): Models of cloud-topped mixed layers under a strong inversion. Quart.J.Roy.Met.Soc.94, 292-309
- Ling, S.C., and Kao, T.W. (1976): Parameterization of the moisture and heat transfer process over the ocean under white-cap sea states. J.Phy.Ocean. 6, 306-315
- Mahrt, L. (1972): A numerical study of coupling between the boundary layer and free atmosphere in an accelerated low-latitude flow. J.A.S.29, 1485-1495
- Miles, J.W. (1957): On the generation of surface waves by shear flow. J.Fluid Mech.3, 185-204
- Miller, B.I. (1964): A study of the filling of Hurricane Donna (1960) over land. Month.Weath.Rev.92, 389-406
- Miyake, M., Doneland, M., McBean, G., Paulson, C.A., Badgley, F., and Leavitt, E. (1970): Comparison of turbulent fluxes over water determined by profile and eddy correlation technique. Quart.J.Roy.Met.Soc.96, 132-137
- Monterieff, M.W. and Miller, M.J. (1976): The dynamics and simulation of tropical cumulonimbus and squall lines. Quart. J.Roy.Met.Soc.102
- Le Mone, M.A., and Pennell, W.T. (1976): The relationship of trade wind cumulus distribution to subcloud layer fluxes and structure. Month.Weath.Rev. 104, 524-539
- Ostapoff, F., Shinnars, W., and Augstein, E. (1970): Some tests on the radiosonde humidity error. NOAA Techn.Rep. ERL 194 - AOML 4, 50 pp

- Ostapoff, F., Tharbeyev, Y., and Worthem, S. (1973): Heat flux and precipitation estimates from oceanographic observations. *Science* 180, No.4089, 960-964
- Paulson, C.A., Leavitt, F., and Fleagle, R.G. (1972): Air-sea transfer of momentum, heat and water determined from profile measurements during BOMEX. *J. Phys. Ocean.* 2, 487-497
- Pennell, W., and Le Mone, M.A. (1974): An experimental study of turbulence structure in the fair-weather trade wind boundary layer. *J. Atm. Sciences* 31, 1308-1323
- Pond, S., Phelps, G.T., Paquin, J.E., McBean, G. and Stewart, R.W. (1971): Measurements of the turbulent fluxes of momentum, moisture and sensible heat over the ocean. *J.A.S.* 28, 901-917
- Reed, R.J., and Recker, E.E. (1971): Structure and properties of synoptic scale wave disturbances in the Equatorial Western Pacific. *J. Atm. Sciences* 28, 1117-1133
- Sarachick, E.S. (1974): The tropical mixed layer and cumulus parameterization. *J.A.S.* 31, 2225-2230
- Sasamori, T. (1972): A linear harmonic analysis of atmospheric motion with radiative dissipation. *J. Met. Soc. Japan* 50, 505-518
- Seguin, W.R., and Garstang, M. (1976): Some evidence of the effects of convection on the structure of the tropical sub-cloud layer. *J. Atm. Sciences* 33, 660-666
- Sheppard, P.A., Tribble, D.T. and Garrett, J.R. (1972): Studies of turbulence in the surface layer over water (Lough Neagh). Part 1 Instrumentation, programme, profiles. *Quart. J. Roy. Met. Soc.* 98, 627-641
- Smith, S.D. (1967): Thrust-anemometer measurements of wind velocity spectra and of Reynolds stress over a coastal inlet. *J. Mar. Res.* 25, 239-262
- Smith, S.D., and Banke, E.G. (1975): Variation of the sea surface drag coefficient with wind speed. *Quart. J. Roy. Met. Soc.* 101, 665-673
- Sommeria, G. (1976): Three-dimensional simulation of turbulent processes in an undisturbed trade wind boundary. *J. Atm. Sciences* 33, 216-241
- Tennekes, H. (1973): A model for the dynamics of the inversion above a convective boundary layer. *J. Atm. Sciences* 30, 558-567
- Tennekes, H. (1973): A model for the dynamics of the inversion above a convective boundary layer. *J. Atm. Sciences* 30, 558-567

- Thompson, N. (1973): An investigation of turbulence structure and fluxes over the sea by a tethered balloon technique. Ph.D. Thesis, Imperial College, London (unpublished)
- Thompson, N. (1974): Convection over the sea. Turbulence and Diffusion Note, Nr. 56, unpublished Techn. Rep. of the Met. Office
- Volkov, J.A., and Kitaigorodsky, S.A. (1967): Some experimental results of statistical characteristics studies of air turbulence and wind waves. IUGG Assembly Bern 1967, Abstracts of papers Vol. 5, JAPO
- Warner, J. (1971): Observations of eddy fluxes of heat and water vapour over the sea. Quart. J. Roy. Met. Soc. 97, 540-547
- Weiler, H.S. and Burling, R.W. (1967): Direct measurements of stress and spectra of turbulence in the boundary layer over the sea. J.A.S. 24, 653-664
- Wucknitz, J. (1976): Determination of turbulent fluxes of momentum and sensible heat from fluctuation measurements and the structure of wind field above waves at the tropical Atlantic during ATEX. Meteor Forsch. Ergeb. B 11 (in print)
- Yanai, M., Espensen, S., Chu, J.H. (1973): Determination of tropical cloud clusters from large scale heat and moisture budgets. J. Atm. Sciences 30, 611-627
- Zipser, E.J. (1969): The role of organized unsaturated convective downdrafts in the structure and rapid decay of an Equatorial disturbance. J. Appl. Meteor. 8, 799-814